Alma Mater Studiorum - Università di Bologna

SCUOLA DI SCIENZE
Dipartimento di Chimica Industriale “Toso Montanari”

Corso di Laurea Magistrale in

Chimica Industriale

Classe LM-71 - Scienze e Tecnologie della Chimica Industriale

The effect of poly(lactide)-poly(carbonate) based block copolymers on the morphology and crystallization of double crystalline poly(lactide)/poly(ε-caprolactone) blends

Tesi di laurea sperimentale

CANDIDATO

Loris Marinetti

RELATORE

Prof. Daniele Caretti

CORRELATORE

Prof. Alejandro J. Müller

Dott. Matteo Rizzuto

Anno Accademico 2015-2016

ABSTRACT

Block copolymers of poly(lactide) and poly(carbonate) were synthetized in three different compositions and characterized by ^{1}H-NMR and ATR analyses. The compatibilization effect of this copolymers on 80/20 (w/w%) PLA/PCL blend was evaluated. SEM micrographs show that all the blends exhibit the typical sea-island morphology characteristic of immiscible blends with PCL finely dispersed in droplets on a PLA matrix. Upon the addiction of the copolymers a reduction on PCL droplets size is observable. At the same time, a Tg depression of the PLA phase is detected when the copolymers are added in the blend. These results indicate that these copolymers are effective as compatibilizers. The copolymer that acts as the best compatibilizer is the one characterized by the same amount of PLA and PC as repeating units. As result, in the blend containing this copolymer PLA phase exhibits the highest spherulitic growth rate. An analyses on PLA phase crystallization behaviour from the glassy state within the blends was evaluated by DSC experiments. Isothermal cold crystallization of the PLA phase is enhanced up an order of magnitude upon blending with PCL. Annealing experiments demonstrated that the crystallization of the PCL phase induces the formation of active nuclei in PLA when cooled below Tg. When the crystallization rate of PCL is retarded, a reduction on PLA nucleation is observed.

SUMMARY

1 INTRODUCTION

1.1 Crystallization of polymers

The crystallization of polymers is a dynamic transition from a highly disordered random state, known as the amorphous phase, into ordered three/two-dimensional crystals built up from folded polymer chains, known as lamellae. A crystalline polymer is composed by a part of molecules organized in regular crystalline phase surrounded by molecules arranged in a random state that conforms the amorphous matrix. The size, number, structure and perfection of these crystals depends on the previous thermal history of the polymer and processing conditions such as: crystallization temperature, composition and molecular weight of the polymer. Generally, a complete crystallization of the polymers chains is impossible to achieve and thus, depending on the crystallinity degree, the proprieties of a crystallizable polymer can be intermediate between those of the perfectly ordered material and the completely amorphous one.

The relative amount of crystalline phase can strongly influence the polymer proprieties, particularly the mechanical one. Since the polymer chains are more closely packed in the crystalline domains, there are more of them available per unit area to support a stress. Thus, crystallinity can significantly increase the strength and rigidity of a polymer. The degree of crystallinity can also influence the optical proprieties of a polymer. In a crystalline polymer, the usually denser crystalline areas have a higher refractive index than the amorphous areas, so crystalline polymers are either opaque or translucent because light is scattered as it passes from one phase to other. So, in general, transparent polymers are completely amorphous and became more opaque as the degree of crystalline phase increase [1]. Furthermore, the degree of crystallinity is a crucial factor affecting the biodegradability of a polymer since enzymatic degradation initially occurs in the amorphous regions, and subsequently in the crystalline regions [2]. The molecules in the amorphous region are loosely packed, and thus are more susceptible to degradation. On the other hand, the crystalline part of the polymers is more resistant to chemical or enzymatic attack and, thus, it can tune the degradation rate of a polymer.

In recent years, there have been several publications dealing with the crystallization of polymers under isothermal and non-isothermal conditions. As well known, crystallization constitutes one of the most important steps in the overall shaping process of semicrystalline polymers.

1.2 Crystallization kinetic

The development of polymer crystallization requires two consecutive steps: the formation of nuclei in the amorphous phase (primary crystallization) and the subsequent growth by self-assembling of more and more polymer molecules (secondary crystallization). The nucleation of a crystal can be defined as the formation of a small amount of crystalline material that occur from a small group of aligned chains segments. Considering that to initiate the formation of a stable nuclei the melt has to be supercooled, it can be established that the greater is the degree of supercooling, the more favourable will be the thermodynamic conditions for nuclei generation [5]. Taking in consideration the site where the nucleation occurs in the amorphous phase, nucleation can be divided into homogeneous nucleation and heterogeneous one. Homogenous nucleation occurs if no second surface or existing nuclei is present and, thus, the nuclei formation takes place spontaneously only due to the supercooling. Heterogeneous nucleation occurs at the surface of impurities within the system and, thus, it requests less supercooling to take place [3]. Generally, primary nucleation is commonly produced in most commercial polymers by heterogeneous nuclei, that is, any particle with the correct size and surface-like as catalytic residues and other impurities of unknown origin [1].

On the other hand, taking in consideration how the nuclei are formed, it can be defined two extremes types of nucleation depending on the crystallization temperature:

1) Instantaneous nucleation occurs when there are many spherulites of small size due to the formation of many nuclei in the same instant. It is obtained to high supercooling where the nucleation rate is greater than the growth rate of the crystals.

2) Sporadic nucleation occurs when the growth rate is higher than the nucleation rate. In this case a few large spherulites are formed when low values of supercooling are employed [4].

The subsequent continuation of crystallization on the growth surface (secondary crystallization) is mainly influenced by the molecular transport: it can only proceed in a temperature range limited on the low temperature side by the glass-transition temperature (Tg) and on the high temperature side by the equilibrium melting point (Tm°) [3]. Below Tg the mobility of the polymer chains is hindered due to the high viscosity, while in the proximity of Tm^0 the chains mobility is too high preventing their assembly.

The trend of the nucleation rate (I) and crystalline growth (G) with the temperature, which is generally of a bell-shaped curve, is shown in Figure 1.1 [5]. The curves are delimited at low temperature from the Tg due to the low molecular mobility and at high temperature from the Tm. As asserted, the spherulitic growth rate is mainly governed by the chains mobility, while nucleation could be affected by the crystallization temperature and the density of heterogeneities present in the melt.

The overall crystallization rate is given by the superposition of both primary nucleation and crystal growth curve as shown in Figure 1.2. The rate of crystallization depends on the crystallization temperature and reach a maximum when a certain value of supercooling ($\Delta T = Tm^0 - Tc$) is achieved. At temperatures

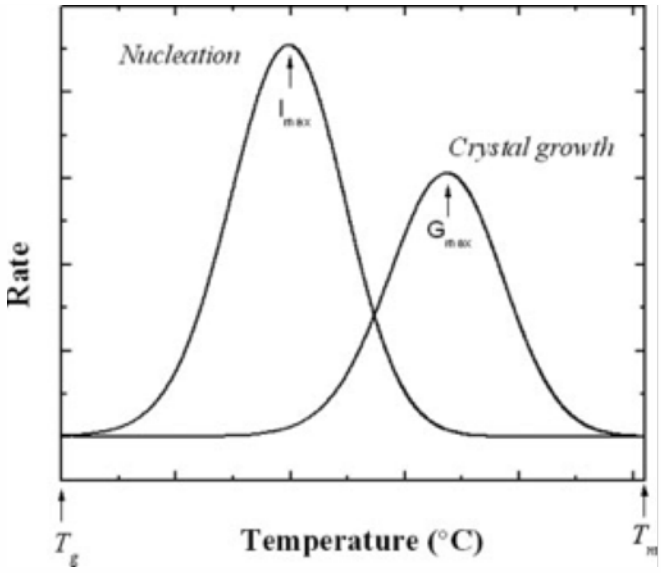

Figure 1.1: Schematic plots for the primary nucleation rate (I) and crystal growth rate (G) as a function of the isothermal crystallization (or nucleation) temperature. Adapted from Lorenzo and Müller [5]

near to the melting, crystallization rate is very low and the process is controlled by nucleation, which is hindered at high temperatures. Lowering the temperature, the

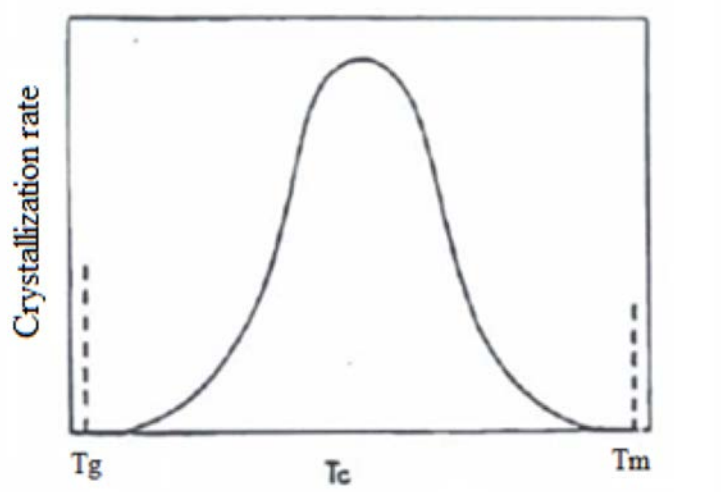

Figure 1.2: Overall crystallization rate as a function of the crystallization temperature.

crystallization rate increases gradually and returns decrease when the crystallization is controlled by diffusion, which is hindered at low temperature.

1.2.1 Avrami theory

The Avrami analysis is one of the most common methods for obtain information about the crystallization kinetics of a polymer [6]. The data obtained during the isothermal crystallization experiments by DSC can be fitted by the Avrami equation which can be expressed as follows [7]:

$$1 - Vc(t - t_0) = \exp[-k(t - t_0)^n] \qquad \text{Eq. (1)}$$

where t is the experimental time, t_0 is the induction time, V_c is the relative volumetric transformed fraction, K is the overall crystallization rate constant and *n* is the Avrami index that is related to both crystals growth and nucleation. Important information about how the nucleation occurs and the crystals morphology can be obtained by the *n* index. The nucleation contribute to the Avrami index (n_n) could be 0 when instantaneous nucleation takes place or 1 for sporadic nucleation. Plotting the Avrami index in function of the crystallization temperature a decreasing behavior is generally obtained as the nucleation became more instantaneous as the temperature increase. The contribute of the crystals growth (n_g) could be 1, 2

or 3 depending on whether one, two or three-dimensional growth occurs and thus can give an indication about the morphology of the crystals (i.e.: sperulitic, disk-line, rod-like…).

The sum of these two contributions (n_n+ n_g) gives the number of Avrami index *n*. To calculate Vc, the following equation can be used:

$$Vc = \frac{Wc}{Wc + \frac{\rho_c}{\rho_a}(1 - Wc)} \qquad \text{Eq. (2)}$$

Since *Wc* is the mass fraction of crystalline, ρ_c the material 100% crystalline density and ρ_a the material 100% amorphous density. The traditionally methods employed for measuring the crystalline fraction, *Wc*, have been the direct volume measurements and DSC experiments in which the fraction Wc is calculated from:

$$Wc = \frac{\Delta H_{(t)}}{\Delta H_{TOT}} \qquad \text{Eq. (3)}$$

where $\Delta H_{(t)}$ corresponds to the enthalpy of crystallization as a function of the crystallization time and ΔH_{TOT} is the maximum crystallization enthalpy of the material. Applying the logarithmic properties on both sides of the equation (1), the following equation can be obtained:

$$\log\left[-\ln\left(1 - Vc\right)\right] = \log\left(k\right) + n log(t - t_0) \qquad \text{Eq. (4)}$$

Plotting $\log\left[-\ln\left(1 - Vc\right)\right]$ as a function of $\log\left(t - t_0\right)$ the values of *k* and *n* can be obtained. An important value that is possible to obtain by the Avrami theory is the half-crystallization time (defined as the time required to attain half of the final crystallinity) indicated as $\tau^{1/2}$ or $\tau_{50\%}$. It is possible to calculate it through this equation:

$$\tau^{1/2} = \left(\frac{-\ln\left(1 - Vc\right)}{k}\right)^{1/n} = \left(\frac{-\ln\left(0.5\right)}{k}\right)^{1/n} \qquad \text{Eq. (5)}$$

1.3 Poly(lactic acid) (PLA)

Poly(lactic acid) (PLA) is one of the well-known biodegradable and bio based polymers, it is a thermoplastic, high-strength and high-modulus material that can be made from renewable resources to form applicable products with traditional processing equipment [8-9-10]. The basic building block of PLA is lactic acid that is mainly produced with two methods: chemical synthesis from petrochemical feedstock and bacterial fermentation of carbohydrates. Nowadays, the majority of the world's commercially produced lactic acid is made by bacterial fermentation of natural feedstocks containing carbohydrates (rice, corn etc.) [11].

The synthesis of poly lactic acid can follow two routes of polymerization: the first, directly from the lactic acid, gives the "*poly-lactic acid"* while the second, indirectly from the lactide (a cyclic dimer of lactic acid), gives the "*polylactide"*. The overall synthesis methods for PLA are depicted in Fig. 1.3 [12-13]. The first route occurs with a polycondensation of lactic acid that yields a low molecular weight polymer which is unusable for any application. As a consequence, external

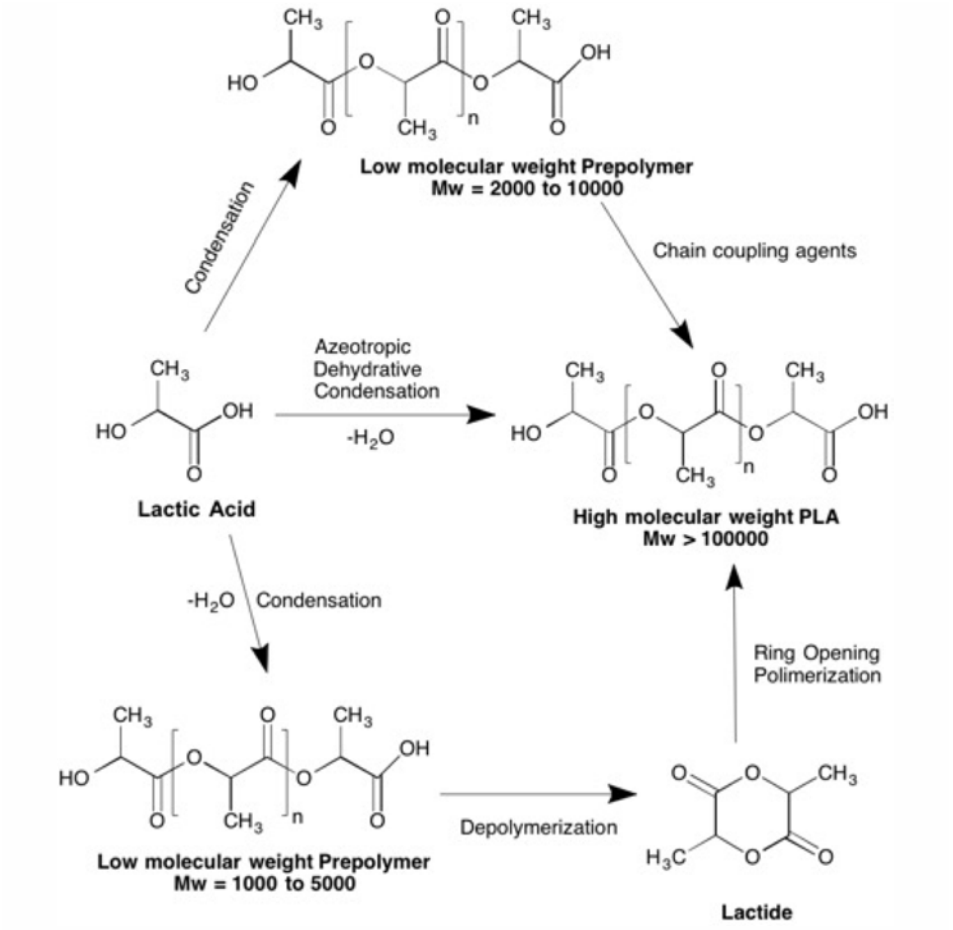

Figure 1.3: Synthesis routes for PLA [12-13]

esterification agents or an azeotropic polycondensation are used to increase the molecular weight [14]. However, these routes are high-expensive and requires long process times due to the high number of intermediate stages and subsequent purifications. On the other hand, the most common method to obtain high-molecular weight PLA starts from lactide that is polymerized with a ring-opening polymerization (ROP) to obtain high-molecular weight PLA. The reaction requests a low-molecular weight PLA as pre-polymer that is then depolymerized to form the lactide.

Lactic acid is the simplest hydroxyl acid with an asymmetric carbon atom and exists in two optically active configurations: the L-(+) and D-(-) isomers. Lactide is obtained by the depolymerization of low-molecular weight PLA to give a mixture of L-lactide, D-lactide and *meso*-lactide as shown in Fig. 1.4. The different percentages of the lactide isomers obtained depends on the lactic acid isomer feedstock, temperature and catalyst [12]. During the synthesis, both isomers give rise to four morphologically different polymers: the polymers coming from pure L- or pure D- feed are referred to PLLA and PDLA respectively, the racemic PDLLA is due to the random distribution of the isomers in the macromolecular chains that gives an amorphous polymer and, finally, the *meso*-PLA that is obtained from DL-lactide.

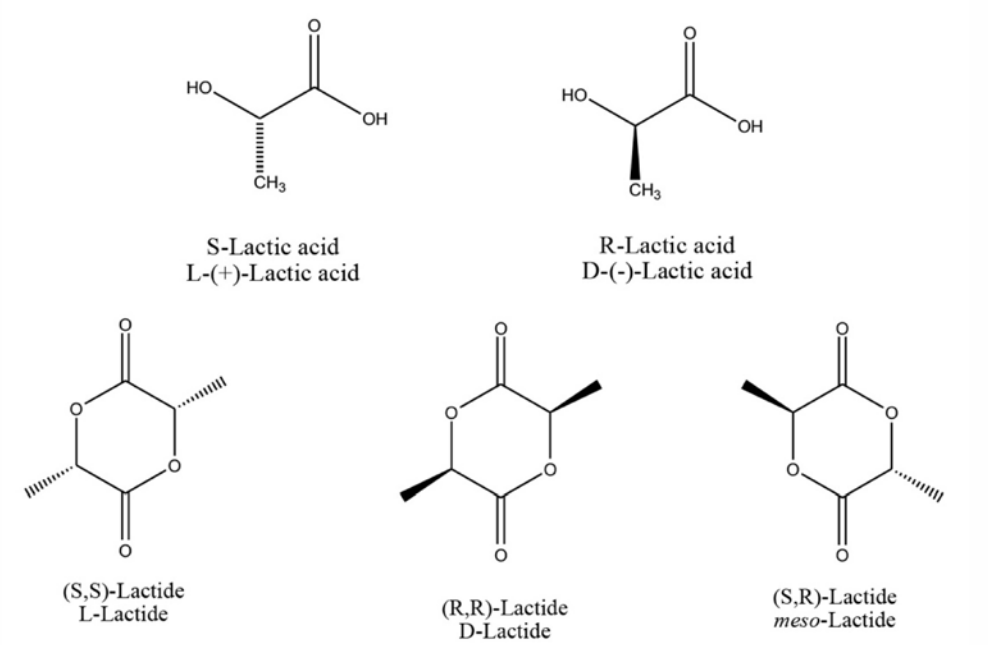

Figure 1.4: Stereochemistry of lactic acid and of the corresponding lactide.

Processing, crystallization, and degradation behaviour of PLA all depend on the structure and composition of the polymer chains, in particular the ratio of the L- and D -isomer of lactic acid influence significantly the resulting proprieties of the material [10]. PLA made from pure L-lactide, also called poly(L-lactide) PLLA, is a semi-crystalline material with an equilibrium melting point of 207 °C and a glass transition temperature about 60 °C [15]. The introduction of stereochemical defects into PLLA (i.e. *meso*-lactide or D-lactide incorporation) reduces the melting point, the rate of crystallization and the extent of crystallization of the polymer [16]. After roughly 15% incorporation of meso-lactide or D-lactide the resulting polymer became amorphous [17]. In order to obtain high-crystalline PLA, stereochemically pure lactic acid is needed but, unfortunately, not all microorganisms yield such stereochemically pure lactic acid and some even produce a racemic mixture that is difficult to separate [10].

PLA materials have been finding an increasing number of applications in the packaging industry due to its good mechanical proprieties, transparency and compostability [10]. However, there are still some drawbacks that restrict the applications of PLA materials. For instance, PLA is a brittle polymer (Tg = 60°C) with a very low impact strength, short extensibility and with a low crystallization rate.

As previously assets, the stereochemical composition of the polymer has a dramatic effect upon the crystallization ability of PLA. Normally, commercial PLA contain pronominally L stereo-isomers units and a minor proportion of D units that acts as stereochemical defects able to hinder the crystallization of L segments within the chains. Indeed, as reported in literature [17-18], the overall nucleation and crystallization rates are inhibited by the presence of D-units that, depending on composition, can lead to the formation of an amorphous polymer.

However, it has been reported that the cold crystallization rate of PLA can be improved with a physical aging at temperatures above the Tg (PLA Tg = 60 °C) that promote a significant increase in the nucleation rate and number of nuclei [19]. When PLA is cooled from the melt state to the glassy state, the molecular mobility slows down, the segments are frozen and the material becomes a thermodynamically unstable glass [20]. Then, from this non equilibrium glassy state, the material will tend to reach an equilibrium state trough slow chains rearrangements that lead to the generation of ordered domains. The domains

formed during physical aging can persist above Tg to some extent and thus act as nuclei to promote the subsequent cold crystallization during heating.

1.3.1 Ring Opening Polymerization of the lactide

The Ring Opening Polymerization (ROP) of the lactide is a method that allows to obtain high molecular weights PLA, above than 100.000 $\overline{M_w}$ [9] due to the possibility of an accurate control of the chemistry and, thus, varying the properties of the resulting polymers in a more controlled manner [10]..

The polymerization mechanism involved in ROP can be induced by different classes of initiators (anionic, cationic, radical), and catalytic systems (enzymatic, organocatalytic etc.). Ring-opening polymerization on lactide generally requires an initiator and in most cases proceeds by chain mechanism which involves sequential additions of monomer to anionic active centres. In the first stage of the polymerization process the lactic acid is purified and converted into a low molecular weight pre-polymer. This pre-polymer is then depolymerized with a catalyst to form a mixture of D-lactide, L-lactide and meso-lactide, which is purified through distillation from residual monomer and catalyst. The purified lactide is then polymerized in a ring-opening reaction using a Tin-based catalyst trough a *coordination-insertion* mechanism shown in Figure 1.5. Tin (II) octanoate ($Sn(Oct)_2$) is the most common catalyst used thanks to its solubility properties,

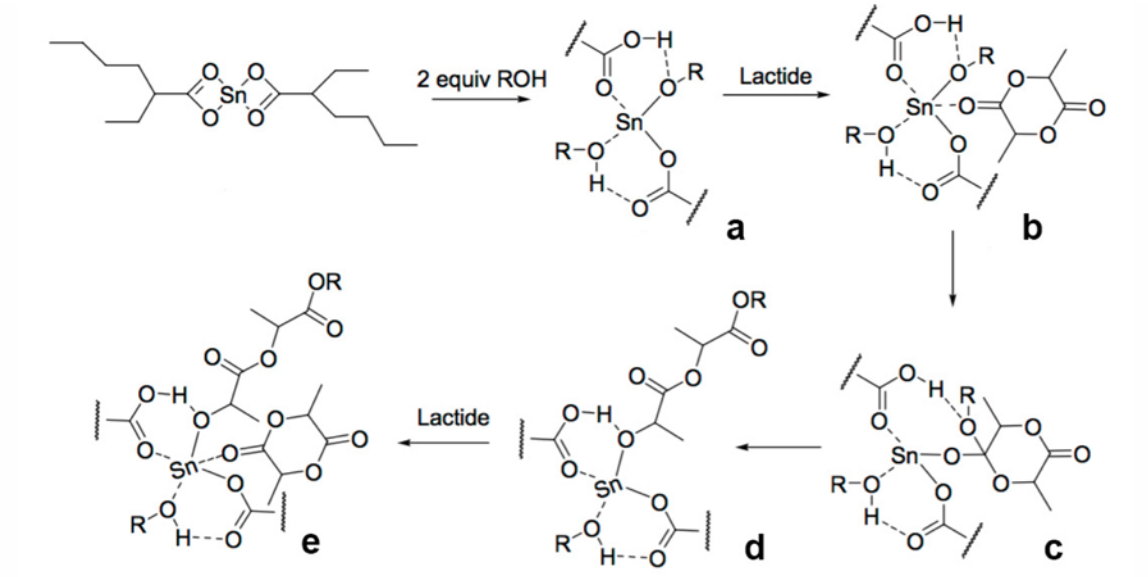

Figure 1.5: Coordination-insertion mechanism of $Sn(Oct)_2$ in catalyzed polymerization of L-lactide.

high catalytic activity and ability to favour the formation of high molecular weight polymers with low levels of racemization (<1%) [21].

The reaction mechanism is shown in Figure 1.5**.** The ROP of lactide is thermodynamically driven by the increase of entropy obtained upon ring opening through an increase of conformational freedom [22].

Molecular modelling suggests that two molecules of an alcohol (ROH) exchange with the octoate ligands (1.5a) followed by the coordination of lactide to the metal centre (1.5b). The Insertion of the alcohol followed by ring-opening (1.5d) generates a linear monomer that subsequently starts propagation (1.5e).

1.4 Polycarbonate (PC)

Polycarbonates are a special class of polymers derived from carbonic acid. Polycarbonates are the second largest by volume engineering thermoplastics known for useful properties such as high heat capability, optical clarity, and incredible toughness [23]. The polycarbonate from bisphenol A (BPA), shown in Figure 1.6, is the most commonly commercialized polycarbonate due to unique characteristics including optical clarity, a relatively high softening temperature (glass transition temperature, Tg ~ 145°C) and remarkable impact toughness [23].

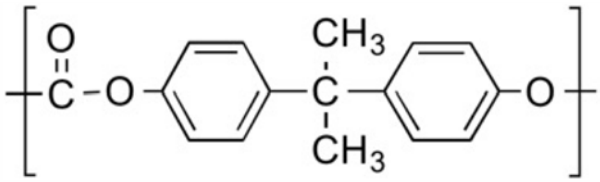

Figure 1.6: Structure of Bisphenol-A polycarbonate

Two very different processes are mainly used for the production of bisphenol A polycarbonate: the interfacial phosgenation and the melt transesterification. The interfacial phosgenation (Fig. 1.7a) involves bubbling phosgene into a solution of bisphenol A in pyridine and isolation of the resulting polymer by precipitation in water or methanol [24]. Although use of phosgene may not be convenient on a laboratory scale due to its toxicity, the large scale use is routine in the chemical industry [23]. On the other hand, in the melt process (Fig. 1.7b) the bisphenol-A is reacted with diphenyl carbonate using a basic catalyst, leading to

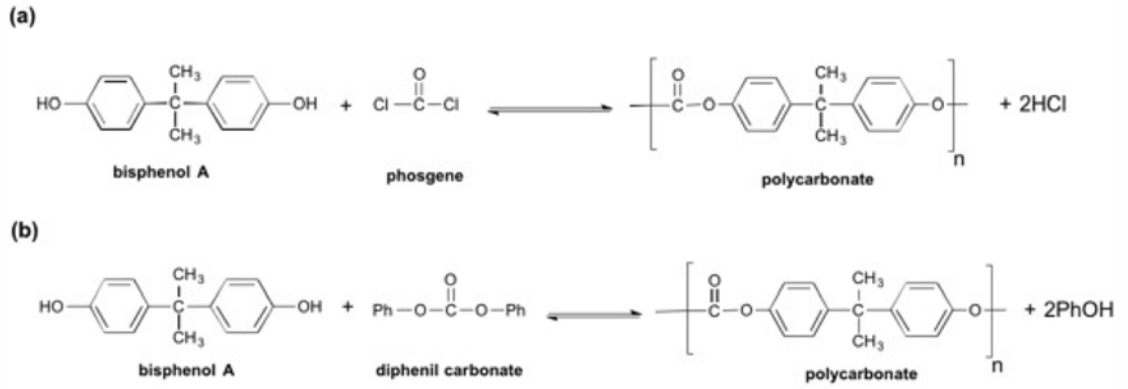

Figure 1.7: General synthesis of BPA-PC polymers

transesterification, with cleavage of phenol which is removed via distillation. Diphenyl carbonate can be prepared either directly, from phosgene and phenol, or by a multistep transesterification process from dimethyl carbonate. Since dimethyl carbonate can be made directly by carbonylation of CO, the melt process can provide a phosgene-free synthesis of polycarbonate [23].

Because of its ability to be modified and tailored to specific applications, the polycarbonates are well used as additive to tune the propriety of other polymers. Blended with miscible polymers, PC can improve the resulting mechanical proprieties of the material (i.e. ABS/PC blends [25]) while it can acts as a nucleation agent when is blended with a second immiscible polymer (i.e. PP/PC [26]).

1.5 Poly(lactic acid) (PLA) – Polycarbonate (PC) *block* copolymers

PLA has been copolymerized with a variety of polymers including polyesters, polyolefins, and natural polymers in order to produce novel materials with various properties. Chemical copolymerization is a very important way to modifying properties of PLA to give new materials with tuneable properties prepared by selection of co-monomers and the variation of copolymer compositions [10]. Indeed, physical properties such as glass transition temperature (Tg), melting temperature (Tm), crystallinity, and mechanical properties can be significantly affected by modifications. Several polymerization techniques can be adopted such as condensation polymerization, ring opening polymerization (ROP), and chain-extension reactions [35].

Among PLA-based copolymers, the interest in poly(lactic acid) (PLA)-poly(carbonate) (PC) copolymers increase in industry for the high performances of polycarbonate and the biodegradability of poly(lactic acid). However, reports about the direct transesterification reactions between PLA and PC have not be reported [27].

Depending on the copolymer composition is possible to modify the proprieties of the resulting material in order to extend its applications. As an example, choosing adequately the design and composition of the copolymers is possible to employ them as compatibilizers for immiscible PLA-based blends. A detailed description of the effect will be described below.

1.6 PLA blends

One of the most promising way to modify the properties of PLA based materials is the physical blending with other polymers. The properties of the resulting polymer blends are tuneable through the choice of blending partners and the change of blend compositions.

A blend of two polymers can be characterized as miscible or immiscible, depending on the number of favourable specific interactions the two components could form a homogeneous single phase or a phase-segregation into individual domains.

The state of miscibility between two polymers is governed by the free energy of mixing, ΔG_{MIX}, which is defined as:

$$\Delta G_{MIX} = \Delta H_{MIX} - T\,\Delta S_{MIX} \qquad \text{Eq. (6)}$$

where ΔH_{MIX} and ΔS_{MIX} are the enthalpy change and entropy change by mixing, respectively [28]. The two polymers are miscible if ΔG_{MIX} is negative, while immiscible if not. In a miscible behaviour, ΔG_{MIX} can only be negative when ΔH_{MIX} is negative so the mixing has to be exothermic, which requires strong interactions between the blend components. Unfortunately, usually only weak van der Waals interactions exist between most polymers, which explains why various existing polymers are fully immiscible.

In order to assess the compatibility between two macromolecules, several parameters based on the free energy of mixing theory can be used. The solubility parameter predicted by the Huggins-Flory theory is an important way to predict the mixing ability between the component of a blend [38], however this parameter is not sufficient to achieve the polymer-polymer miscibility due to specific interactions between the polymers chains that are not considered in this thermodynamic treatment. Consequently, the miscibility of a polymer blend can be also evaluated from experimental evidences obtained studying mainly the morphology and the glass transition temperature (Tg) of the blend. A completely miscible blend exhibits a homogeneous morphology with a single Tg, which is between the Tg values of both components and changes with the composition while an immiscible blend usually exhibits a macrophase-separated morphology with two Tg values, which are independent of blend compositions.

Since PLA is a brittle polymer with a high Tg (nearly 60 °C), the blending with plasticizers or with miscible and more flexible polymers is a simple and efficient method to reduce its glass transition temperature due to the plasticization effect which enhance the mobility of PLA chains. In this way it is theoretically possible to modify the thermal and mechanical proprieties of PLA materials in order to extend their applications.

For this purpose, a large number of miscible and immiscible PLA-based blends have been exhaustively investigated. For instance, Nijenhuis et al. reported that miscible blends of PLA with poly(ethylene oxide), PEO, exhibit a single Tg value that changes with the PLA/PEO composition (according with the Fox-Flory equation (Eq.11)) and an increase of the PLA crystallization ability in isothermal condition is observed [29]. As the PEO content of the blend increase an increasing in the PLA heat of fusion is observed and the melting peaks of PLA phase are shifted at lower temperature compared with neat PLA. It is also reported that blending PLA with poly(ethylene glycol) PEG promote the crystallization of PLA by improving the mobility of PLA chains (plasticizer effect) and thus accelerating its crystallization rate. So, PEG addiction enhance the crystallization of PLA phase upon cooling and allows PLA to crystallize at higher temperatures [30].

1.7 Poly(L-lactide) (PLA)/Poly(ε-caprolactone) (PCL) blends

PLA/PCL blend is one of the most extensively investigated blends of biodegradable polymers due to the mechanical performance and the bio-compatibility of the obtained polymeric system.

PCL is a biodegradable, biocompatible and semi crystalline polyester with low melting point and glass transition temperature (Tm = 60 °C, Tg = -60 °C) [31]. At room temperature PCL presents low tensile modulus and high elongation at break while PLA shows high modulus and low elongation at break due to it is higher glass transition temperature [32]. Since PCL is much more flexible polymer, the blending with PLA could compensating certain undesirable characteristic of PLA such as brittleness and low flow rate for processing [33]. Although in PLA/PCL blends the mismatch between the solubility parameters is not large (10.1 ($cal^{0.5}/cm^{1.5}$) for PLA and 9.2 ($cal^{0.5}/cm^{1.5}$) for PCL), there are no specific interaction between the polymer chains that can induce miscibility [34]. In fact, the immiscibility of PLA/PCL blends has been well reported in literature by morphological and thermal evidences [32,58,43,59].

For incompatible polymer blends such as PLA/PCL several compatibilization strategies can be followed in order to improve the miscibility between the two phases and, thus, enhance the properties of the blends (i.e. addition of copolymers, addiction of reactive polymers with functional groups, addition of low molecular weight chemicals etc.) [35]. The most important roles of compatibilization are first to reduce the size of the dispersed phase through the reduction of interfacial tension and second to prevent the coalescence of the dispersed phase stabilizing the formed phase morphology [36].

The addition of copolymers is a conventional and efficient way to compatibilize polymer blends due to the higher compatibilization efficiency and the lower cost as compared to the other compatibilization methods. The most widely used copolymers are those which have blocky structures with one constituent block miscible with one phase of the blend and a second block miscible with the other phase [36]. Figure 1.8 shows a schematic representation of the supposed conformation of block-copolymers at the interface of an immiscible blend.

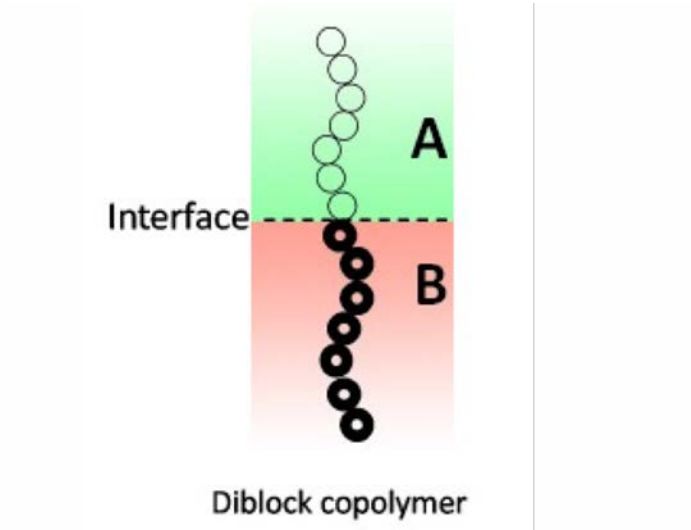

Figure 1.8: Representation of block-copolymers conformation at the interface of an immiscible blend

The presence of block copolymers at the interface can decrease the interfacial tension between the immiscible phases due to the entanglement of each block with the corresponding blend component; this effect promotes the reduction in size of the dispersed phase. An adequate degree of interfacial adhesion is essential for stress transfer from one phase to the other, which is efficient in stopping the cracks initiated at the interface from growth to catastrophic failure. In addition, the existence of the blocky-structured copolymer at the interphase could prevent coalescence of the generated dispersed particles during subsequent processing or storage [36]. The formation and stabilization of a fine phase morphology and the improvement in the interfacial adhesion usually change a useless immiscible blend to a useful material in which the advantages of each blend component are combined [36].

In literature many works were focused on the compatibilization of PLA blends by adding block copolymers. For instance, PLA–PCL diblock or triblock

copolymers have been widely used to compatibilize immiscible PLA/PCL blends. Choi et al. [37] synthesized a PLA–PCL diblock copolymer and used it to compatibilize PLA/PCL blends and found that the size of PCL domains in PLA matrix can be reduced upon addition of PLA–PCL di-block copolymer.

1.8 Crystallization of PLA phase within miscible and immiscible blends

The crystallization of PLA in miscible and immiscible polymer blends can differ remarkably from that of the neat crystallizable PLA.

The crystallization ability of PLA phase when is blended with a miscible polymer can either increase or decrease depending on the effect of composition on the glass-transition temperature of the blend and on the equilibrium melting point of the crystallizable component (plasticization or anti-plasticization effect) [38]. When PLA is blended with a second more flexible and miscible polymer (i.e. PEG, PEO) a reduction on its glass transition temperature is expected according to the Fox-Flory prediction (Equation (11)) due to the plasticization effect that improve the mobility of PLA chains [38]. As a consequence, PLA chains can move easily and thus the PLA crystallization ability is enhanced. This effect is well reported in literature for different types of PLA-based miscible blends [39-40-29]. Otherwise, when PLA is blended with a second miscible and more rigid polymer the chains mobility is reduced respect the bulk polymer and thus an increase in the PLA glass transition temperature is expected (anti-plasticization effect).

On the other hand, in immiscible blends of PLA both phases are physically separated and thus they can exert a significant influence on each other. The presence of the second component can disturb the normal crystallization process of PLA and, thus, can affects crystallization kinetics, spherulite growth rate, semicrystalline morphology, etc. [38]. As an example, several works report that the addiction of an immiscible polymer such as PCL to PLA enhanced the crystallization rate of PLA due to a nucleation effect [41-42-32-43]. Generally, when two immiscible polymers are blended two possibilities may occur to induce nucleation. One component can nucleate the other by promoting nucleating activity at the interface or, during mixing in the melt or solution, a migration of active heterogeneities can occur from one phase to the other [38]. Sakai et al. [42]

proposed that the nucleation effect shown in PLA/PCL blends derives from a locally Tg depression at the PLA/PCL interphase that could induce the formation of active nuclei in PLA phase.

2 OBJECTIVE OF THE THESIS

PLA is one of the most extensively investigated biodegradable polymers derived from renewable resources due to its attractive mechanical and thermal proprieties. However, commercial PLA materials have certain shortcomings that limit their applications. PLA is a brittle and hard polymer with a very low impact strength and low extensibility. In addition, the poor crystallizability, slow biodegradation rate, and low heat distortion temperature are the other shortcomings limiting the wide application of PLA.

One of the most promising way to overcome PLA limits is the physical blending with a selected more flexible polymer. PLA/PCL is a well-extensively studied PLA-based blend since PCL is a biodegradable and biocompatible flexible polymer that can enhance some limits of PLA. PCL is a semicrystalline polymer with low tensile strength, high elongation at break (above 400%), and processing temperatures similar to PLA that has the potential to act as a plasticizing agent in blends with PLA. Nevertheless, the immiscibility between PLA and PCL due to the lack of specific interactions between PLA and PCL chains represent the principal limit of this blend.

In order to enhance the miscibility between PLA and PCL phases an innovative type of block copolymers composed by poly(lactide) and poly(carbonate) were synthetized in different compositions and characterized by spectroscopic analyses (^{1}H-NMR and ATR). The objective of this thesis is to evaluate the compatibilization effect of poly(lactide-*block*-carbonate) synthesized upon blending with poly(lactide)(PLA)/poly(ε-caprolactone)(PCL) 80/20 blend. The miscibility between PLA and PCL upon copolymer addiction was evaluated observing the cryo-fractured SEM micrographs of the samples and the Tg variation of the PLA phase during non-isothermal DSC experiments. The results were correlated with the spherulitic growth rate of PLA phase in the blends evaluated by PLOM experiments. The overall crystallization kinetics (nucleation + growth) of the PLA phase within the blends was investigated by isothermal DSC experiments. In order to deep the previous analyses, annealing DSC tests was performed to elucidate the role of PCL phase on the nucleation rate of PLA.

3 EXPERIMENTAL

3.1 Materials and methods

Poly(L-lactide) (PLA, Ingeo index: 4032D, 1.2-1.6% D-LA isomer, $\overline{M_w}$ = 200 kDa, Tg = 60°C) was purchased from NatureWorks™ and was dried overnight under vacuum at 60°C before processing to avoid degradation reactions induced by moisture. Poly(ε-caprolactone) (PCL, CAPA 6500, $\overline{M_w}$= 45 kDa, Tg= -60°C) was purchased from Solvay™ and was used as received. Policarbonate (PC, TARFLON® IV1900R, Tg = 140°C) was purchased from Idemitsu Chemicals Europe and was used as received. Bisphenol-A (BPA) (Sigma-Aldrich-CAS Number:80-05-7), diphenyl carbonate (DPC) (Sigma-Aldrich-CAS Number:102-09-0) and the L-lactide (Sigma-Aldrich-CAS Number: 4511-42-6) have been previously purified by recrystallization from boiling toluene and subsequent complete elimination of the solvent. Tin octanoate (Sigma-Aldrich-CAS Number: 301-10-0) and NaOH (Sigma-Aldrich-CAS Number: 1310-73-2) were used as received.

Three different kinds of Poly(L-lactide)-Poly(carbonate) block copolymers were used: P(LA-*b*-C)80-20, P(LA-*b*-C)50-50, P(LA-*b*-C)15-85. These copolymers were synthesized by ring opening polymerization using toluene as solvent at 95 °C with stannous(II) octanoate as catalyst (detailed synthesis is described in paragraph 3.2). Composition (LA/C), average molecular weights ($\overline{M_w}$), polydispersity (D) and glass transition temperatures (Tg) of the block copolymers are reported in Table 3.1.

Table 3.1: Composition (LA/C), weight average molecular weights ($\overline{M_w}$), polydispersity (D) and glass transition temperatures (Tg) of the block copolymers.

Sample	LA/C (w/w)[a]	$\overline{M_w}$ (Da)[b]	D[c]	Tg(°C)[d]
P(LA-*b*-C)80-20	80/20	6400	1.4	62
P(LA-*b*-C)50-50	50/50	5200	1.9	74
P(LA-*b*-C)15-85	15/85	5700	2.0	110

[a] Composition weight ratio between Lactide unit (LA) and Carbonate unit (PC) determined by ^{1}H-NMR. [b] Determined by SEC (THF) with PS standard.[c] Determined as Mw/Mn. [d] Determined by DSC, heating curves at 20°C min $^{-1}$

3.2 Synthesis of copolymers

The overall synthesis of P(LA-*b*-C) copolymers is composed by two steps:

- First step: synthesis of poly(bisphenol-A carbonate).

The synthesis of poly(bisphenol-A carbonate) oligomers was performed by melt transesterification process using diphenyl carbonate (DPC) and bisphenol-A (BPA) in molar ratio 1/1. A schematic representation of the reaction is shown in Figure 3.1. The reaction was conducted under vacuum in the presence of NaOH as basic catalyst. Since the equilibrium constant of the reaction approaches unity, removal of phenol from the system is necessary to drive the reaction towards the products [44].

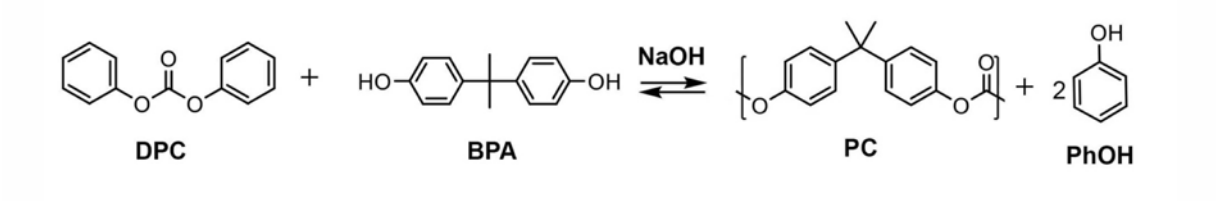

Figure 3.1: Schematic representation of PC oligomers synthesis using DPC and BPA.

Diphenyl carbonate and bisphenol-A with a molar ratio of 1/1 were initially dried in oven and then placed in a three-necked flask. The reactants were melted at 170 °C for 1 hour in presence of NaOH (0.2 mmol) at ambient pressure under nitrogen atmosphere. Subsequently, the nitrogen flow was stopped and the flask was put under stirring in an oil bath at a controlled temperature of 200 °C for 5 hours under vacuum. At the end of reaction, the crude was first diluted with a small amount of dichloromethane to reduce the viscosity and subsequently purified by precipitation with an equimolar mixture of methanol and ethanol. The precipitate was filtered and subsequently dried in a thermostated oven at 60 °C for 24 hours.

- Second step: synthesis of P(LA-*b*-C) copolymers

P(LA-*b*-C) copolymers were synthetized in three different compositions by a bulk ring-opening polymerization (ROP) using purified commercial L-lactide and PC oligomers by changing the LA/PC (w/w%) ratio employed. The composition used are described in Table 3.2 while a schematic representation of the reaction is shown in Figure 3.2 The reaction was carried out in a Schlenk tube using $Sn(Oct)_2$ as catalyst, toluene as solvent and under nitrogen flux. In the first step, the L-lactide and PC were weighted into the Schlenk tube under nitrogen atmosphere whit $Sn(Oct)_2$ (1.5 mmol – 0.5 ml) and toluene (10 ml). The reaction mixture was

frozen by immersion in liquid nitrogen and subsequently immersed in an oil bath at 95 °C for 24 hours under agitation to allow the polymerization. The raw products were dissolved in 50 ml of dichloromethane and then poured into 200 ml of methanol. The precipitation collected by filtration was purified by a reprecipitation with dichloromethane and methanol and finally dried in a thermostated oven at 60 °C for 24 hours.

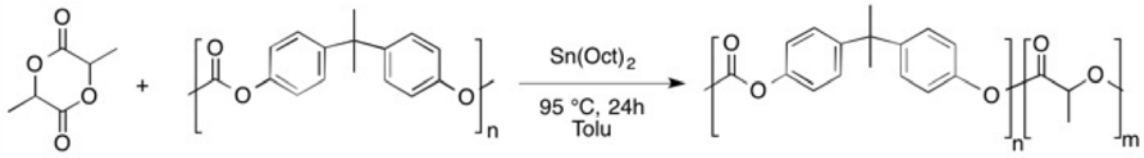

Figure 3.2: Schematic representation of P(LA-*b*-C) syntesis

Table 3.2: Feeding composition of P(LA-*b*-C) copolymers

SAMPLE	LA (g)	C (g)	LA/C (w/w%)
P(LA-*b*-C)80-20	0.8	0.2	4/1
P(LA-*b*-C)50-50	0.4	0.4	1/1
P(LA-*b*-C)15-85	0.2	0.8	1/4

3.3 Blends preparation

A constant PLA/PCL weight ratio of 80/20 was employed since recent studies have shown that the blend offers a well-balanced combination of stiffness and toughness at this composition. [41-45-46-47-48-49]

The P(LA-*b*-C) block copolymers and neat PC were used as compatibilizers, by adding 10% with respect to the minor phase. The approximate final blend composition is 80/20/2 PLA/PCL/Compatibilizer.

In order to study the effect of PC in neat PLA matrix, PLA/PC blends were also prepared at the composition of (w/w%): 99/1, 98/2 and 95/5. (see Table 3.3).

All the blends were prepared by solvent-casting method. Neat materials and the compatibilizers were dissolved in dichloromethane, under the composition presented in Table 3.3, at the concentration of 1 g/dL and stirred at room temperature for 3 hours. The film forming solutions were casted in Petri dishes (diameter = 5 cm). The obtained films were dried for 24 hours at room temperature

Table 3.3: Composition of the prepared blends

Sample name	PLA (w/w%)	PCL (w/w%)	P(LA-*b*-C) 80-20 (w/w%)	P(LA-*b*-C) 50-50 (w/w%)	P(LA-*b*-C) 15-85 (w/w%)	PC (w/w%)
PLA	100	-	-	-	-	-
PCL	-	100	-	-	-	-
PLA/PCL	80	20	-	-	-	-
PLA/PCL/P(LA-*b*-C) 80-20	79	19	2	-	-	-
PLA/PCL/P(LA-*b*-C) 50-50	79	19	-	2	-	-
PLA/PCL/P(LA-*b*-C) 15-85	79	19	-	-	2	-
PLA/PCL/PC	79	19	-	-	-	2
PLA/PC	99	-	-	-	-	1
PLA/PC	98	-	-	-	-	2
PLA/PC	95	-	-	-	-	5

and for another 24 hours at 60 °C under vacuum in order to remove residual solvent.

The morphology of the blends was investigated by Scanning Electron Microscopy (SEM). The blends were cryogenically fractured after 3 hours of immersion in liquid nitrogen. Fracture surfaces were observed after gold coating under vacuum, using a Hitachi S-2700 electron microscope.

Micrographs of the most representative inner regions of the specimens were obtained. PCL droplet diameters were measured on at least 100 particles. Number (dn) and volume (dv) average diameters and particle size polydispersity (D) were calculated by the following equations [50]:

$$d_n = \frac{\sum n_i d_i}{\sum n_i} \qquad \text{Eq. (7)}$$

$$d_v = \frac{\sum n_i d_i^4}{\sum n_i\, d_i^3} \qquad \text{Eq. (8)}$$

$$D = \frac{d_v}{d_n} \qquad \text{Eq. (9)}$$

where n_i is the number of droplets “i” of diameter d_i.

Polarized Light Optical Microscopy (PLOM) was employed to observe the morphology and growth of PLA spherulites. Micrographs were recorded by a

LEICA DC 420 camera on film samples with a thickness of approximately 10 μm, cut from tensile test specimens. By using a METTLER FP35Hz hot stage, the films were firstly held at 200 °C for 3 minutes to erase previous thermal histories, and then they were cooled to the crystallization temperature and the isothermal spherulitic growth was followed by PLOM.

3.4 Spectroscopic Analyses

Spectroscopic analyses were performed on PC oligomers and on P(LA-*b*-C) copolymers by ^{1}H-NMR and ATR experiments. In this work, the ^{1}H-NMR spectra have been recorded with a spectrometer Varian "Mercury 400" operating at 400 MHz on samples were prepared in DMSO solution at the 1.0 wt%. Chemical shifts (δ) for ^{1}H are given in ppm relative to the known signal of the internal reference (TMS).

The ATR spectra were recorded on a Bruker Alpha FT-IR spectrometer. Data were collected with powder sample in ATR mode (Bruker). The spectra were taken in the range of 4000–500 cm^{-1} with a resolution of ± 2 cm^{-1}.

3.5 Thermal analyses

The thermal behaviour of the blends was studied by Differential Scanning Calorimetry (DSC) using a Perkin Elmer DSC Pyris 1 calorimeter calibrated with indium and tin. All measurements were performed under nitrogen atmosphere and using sample masses of approximately 5 mg. The analyses were conducted with different methods as a function of the experiment.

In **non-isothermal analysis** the samples were heated from 25 °C to 200 °C at the rate of 10 °C/min and held at 200 °C for 3 minutes to erase the thermal history. Then they were cooled at 10 °C/min until - 20°C and finally heated at 10 °C/min to 200 °C.

In combined isothermal/non isothermal experiments, the samples were first heated to 200 °C and kept at that temperature for 3 minutes to erase the thermal history. Then they were cooled at 60°C/min (in order to avoid PLA crystallization during cooling) until specific isothermal crystallization temperatures between 54 °C and 0 °C and held at this temperature for 15 minutes. Then the samples were reheated at 20 °C/min to 200 °C.

In **isothermal analysis** the samples were heated from 25 °C to 200 °C at 20 °C/min and held for 3 minutes to erase the thermal history. Then they were cooled at 60 °C/min (in order to avoid PLA crystallization during cooling) to 20 °C and held at this temperature for 1 minute. Then they were heated at 60 °C/min to the crystallization temperatures in a range between 150 °C and 90 °C and held until the crystallization is finished (20 min at least). Finally they were reheated to 200°C again at 20°C/min.

Two kinds of annealing experiments were performed:

Annealing experiment 1: the samples were heated to 200 °C and kept at that temperature for 3 minutes in order to erase thermal history. Then they were cooled at 60 °C/min (in order to avoid PLA crystallization during cooling) until a certain annealing temperatures between 54 °C and 0 °C. Then, the samples were kept at this temperature for 15 minutes and re-heated to 200 °C at 20 °C/min in order to detect the cold crystallization temperature of PLA that occurs in a range between 90 °C and 130 °C.

Annealing experiment 2: the samples were heated to 200 °C and kept at that temperature for 3 minutes in order to erase thermal history. Then they were cooled at 40 °C/min to -10°C in order to crystallize PCL. Then the samples were heated until a certain annealing temperatures between 0 °C and 38 °C in order to avoid PCL melting. The sample were kept at this temperature for 15 minutes and re-heated to 200 °C at 20 °C/min in order to detect the cold crystallization temperature of PLA.

The thermal degradation of the samples was studied by thermogravimetric analysis (TGA). The experiments were performed in a thermobalance TA Instruments, model Q500, constituted by an electronic balance placed inside an oven. Heating scans were performed in an inert atmosphere using high purity nitrogen. For every analysis about 5-10 mg for each sample was used. The analysis were performed keeping the samples for 1 minute at 40°C and heating from 40°C to 600°C at 20°C/min.

4 RESULTS AND DISCUSSIONS

4.1 Characterization of copolymers

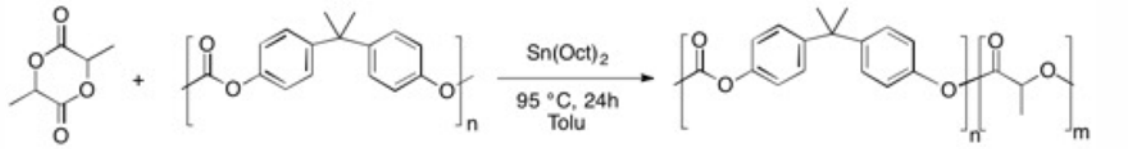

Figure 4.1: Schematic representation of P(LA-*b*-C) copolymers synthesis

P(LA-*b*-C) copolymers were synthetized by a bulk ring-opening polymerization (ROP) using commercial L-lactide and pre-synthetized PC oligomers as shown in Figure 4.1. However, the synthesis of PC and the subsequent polymerization with L-lactide are two different kinds of reactions that requires different temperatures

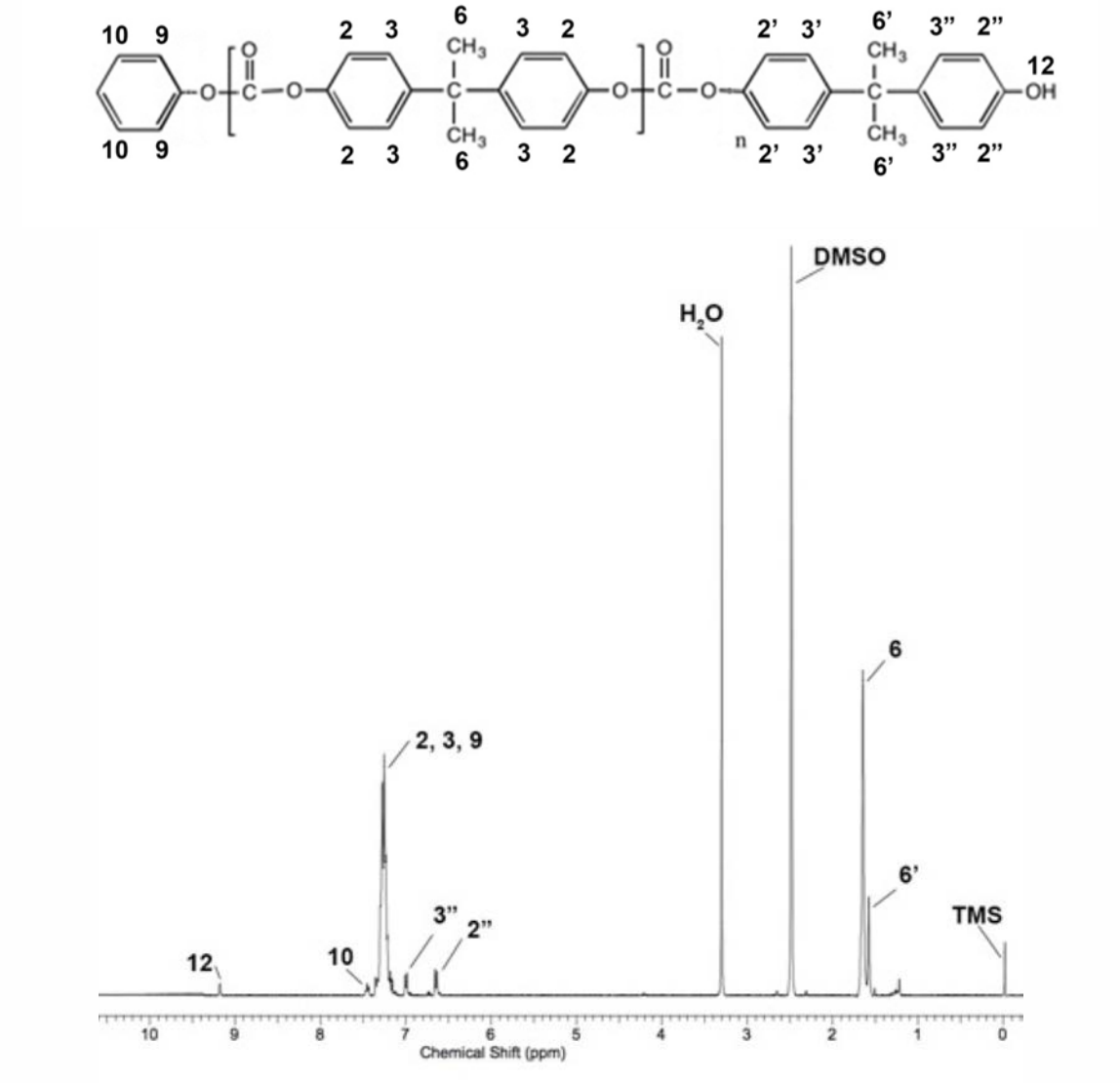

Figure 4.2: ^{1}H-NMR spectrum for PC oligomers recorded in DMSO

and catalysts. Because of these differences, it has been decided to develop the two reactions separately, the procedures employed are well described in paragraph 3.2. The products obtained were characterized by thermal and spectroscopical analyses.

Polycarbonate oligomers were investigated using proton nuclear magnetic resonance (^{1}H-NMR) on the precipitate obtained (Fig. 4.2).

The analysis of the ^{1}H-NMR spectrum was performed using the work of Kim et al. as reference [51]. At 2.5 ppm is observable the characteristics peak of DMSO and at 3.3 ppm is present the peak of residual water. The two singlets at 1.65 ppm and 1.58 ppm are referred to the methyl protons present in the main chain (6) and at the chain end (6') of bisphenol-A unit. The multiplet from 7.1 to 7.4 ppm is referred to the aromatic protons in position (2) and (3) of the polymerized bisphenol-A unit, while the doublets at 6.65 and 7.0 ppm are referred to the aromatic protons in position (2") and (3") of the end chain. The triplet at 7.45 ppm is referred to the two aromatic protons of the terminal aromatic ring (10) while the signal of the two protons in position (9) is overlapped with the aromatic protons in the main chain (3). The signal at 9.16 ppm is related to the proton of the –OH group (peak assignment 12) and suggest the presence of a phenolic chain end. The functional groups at the chain end of the oligomers play a pivotal role for the

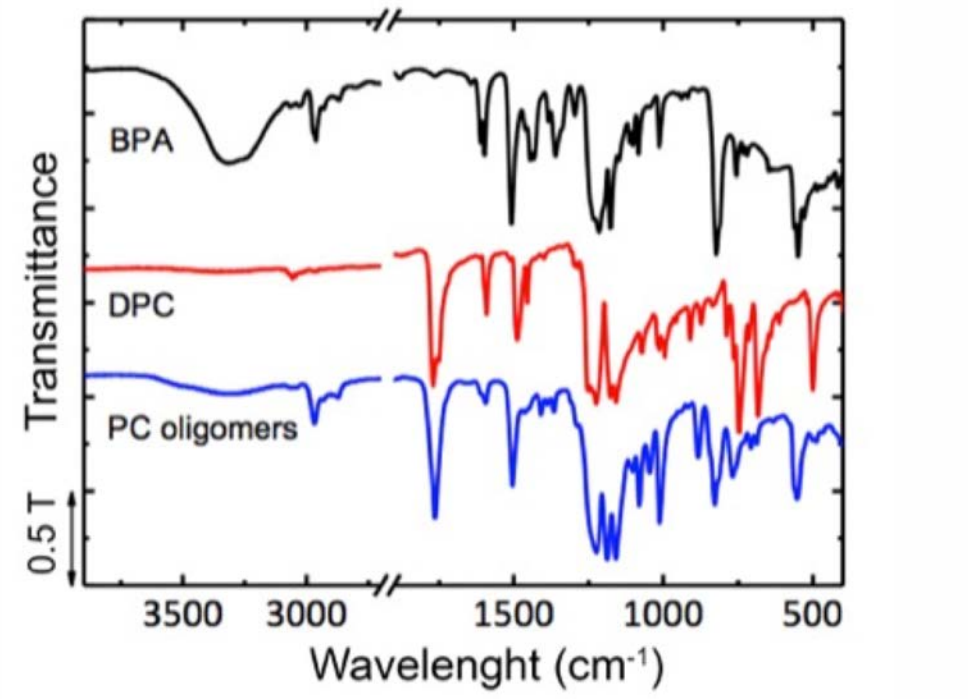

Figure 4.3: ATR absorption spectra of PC oligomers, neat BPA and neat DPC

subsequent polymerization of PC with the L-lactide acting as the initiator of the ring opening polymerization.

ATR experiments on the reaction precipitate were performed in order to investigate the structure of PC oligomers obtained. Figure 4.3 shows ATR spectra recorded for PC oligomers compared with those of neat BPA and DPC. The interpretation of the ATR spectra was performed using the work of Parshin et al. as reference [52]. The ATR spectra of DPC shows a strong absorption band at 1755 cm^{-1} due to the C=O stretching vibration that is also present in the spectrum of PC oligomers. In the spectrum of BPA the high intense band at 3300 cm^{-1} is related to the stretching of the -OH group. This band is also present, less intense, in the spectrum of product synthetized confirming the previous hypothesis about the chain end groups of the PC oligomers. PC oligomers exhibit at about 3000 cm^{-1} the C–H aromatic ring deformations while the symmetric and asymmetric stretching band of C-O-C groups appears in a range that goes from 1000 cm^{-1} to 1270 cm^{-1}.

The thernal behaviour of our bisphenol-A polycarbonate was investigated by DSC experiments. The sample was heated from 25 °C to 200 °C at different scanning rates. In Fig. 4.4 are shown the first heating scans at 10, 20, 40 °C/min.

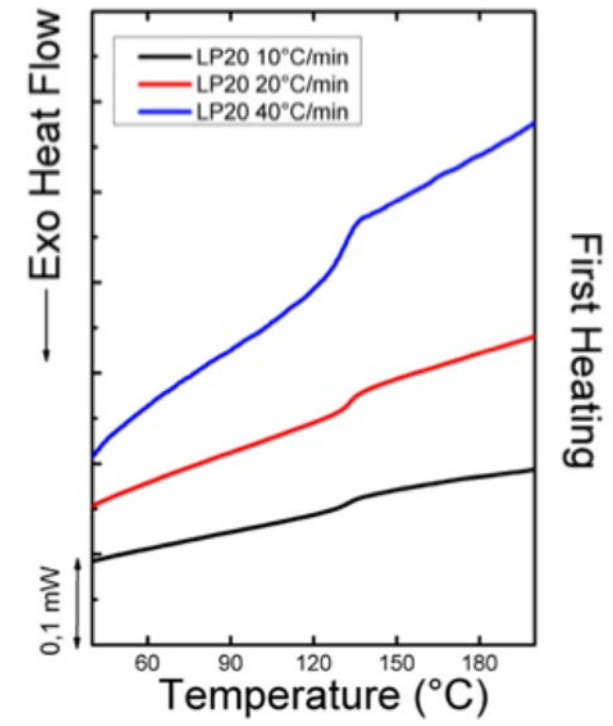

Figure 4.4: DSC experiments for PC oligomers. First heating curves measured at different scanning rates. The curves have been normalized by the weight of the samples

Table 4.1: Values of Thermal transitions obtained from DSC experiments at different scanning rates

Heating Rate	Tg [°C]
10 °C/min	132
20 °C/min	133
40 °C/min	132

Curves obtained for each scanning rate employed show a single glassy-rubbery transition in a temperature range between 130 °C and 135 °C. As reported in Table 4.1, the Tg values obtained are always lower in comparison with the common T_g value of BPA- polycarbonate reported in literature (T_g = 145 °C) [53]. This behaviour is due to the low molecular weight obtained in our polycarbonate oligomers: short polycarbonate chains can moves easily so they requests lower energy contribute to unlock the torsional and rotational movements [54].

PC oligomers synthetized were subsequently polymerized with purified commercial L-lactide trough a ring opening polymerization (ROP) using $Sn(Oct)_2$ as catalyst. The final composition of the poly(lactide-*block*-carbonate) copolymers synthetized was determined by spectroscopic experiments (^{1}H-NMR and ATR). Figures 4.6 (a), (b), (c) show ^{1}H-NMR spectra of P(LA-*b*-C) copolymers recorded in DMSO. The spectra obtained for each copolymer show the same pattern with differences in the intensity of characteristic peaks of both PLA and PC blocks. The analysis of the ^{1}H-NMR spectra was performed using the previous characterization on PC block and the work of Liu et al. as reference [27]

The aliphatic singlet at 1.65 ppm is related to methyl protons of the PC block (1) while the multiplet from 7.1 to 7.4 ppm is related to the aromatic protons of the PC block (2 and 3)**.** The doublet at 1.45 ppm is related to the methyl protons of the PLA block (4) while the quartet at 5.2 ppm is related to the methine of PLA block (5). As shown in Figure 4.6, the intensity of the characteristic signals of both PLA and PC blocks change in proportion with the LA/C content of the copolymers. The final copolymer composition was determined from the weight fraction of PLA block calculated by integration of methine proton of PLA block (5) and integration of aromatic proton of polycarbonate block (peak assignments 2 and 3) at the chemical shifts of 5.25 and 7.2 ppm respectively. The following equation was used:

$$LA\ \left(\frac{w}{w}\%\right) = \left(\frac{I_{LA}}{n_{LA}} \times Mw_{LA}\right) \div \left[\left(\frac{I_{LA}}{n_{LA}} \times Mw_{LA}\right) + \left(\frac{I_{PC}}{n_{PC}} \times Mw_{PC}\right)\right] \qquad \text{Eq. (10)}$$

were I is the intensity calculated by integration of the peaks, n is the number of protons related to the peaks and Mw are the molar weight of PLA and PC repeating units, respectively.

The composition of P(LA-*b*-C) copolymers was investigated by IR spectroscopy. In Figure 4.5 is shown the ATR spectrum obtained for copolymers in comparison with those of neat PLA and neat PC. Neat polycarbonate oligomers exhibit at 3400

cm^{-1} the absorption band of the hydroxyl ending group (-OH) while this signal was not detected among P(LA-*b*-C) copolymers. This behaviour is a direct consequence of the trans-esterification between L-lactide and PC oligomers in which the –OH terminal groups of PC acts as initiator for the reaction and thus are no longer detectable on the products of reaction. P(LA-*b*-C) copolymers exhibit at 1750 cm-1 the stretching band of the carbonyl group (C=O) present in both PC and PLA blocks. Neat PLA and PC exhibit the stretching of the C-O-C group in a range between 1000 and 1270 cm^{-1}. On the spectra of P(LA-*b*-C) copolymers the band related to the stretching of C-O-C group is always observable and exhibit a pattern that change with the LA/C content of the copolymers. In the copolymer with the larger amount of PLA (P(LA-*b*-C)80-20) the stretching band of C-O-C group at 1100 cm^{-1} appears as a single band with a triple peak and the same trend is shown for the spectrum of neat PLA. On the other hand, the copolymer with the highest content of PC (P(LA-*b*-C)15-85) presents at 1100 cm^{-1} the C-O-C stretching band

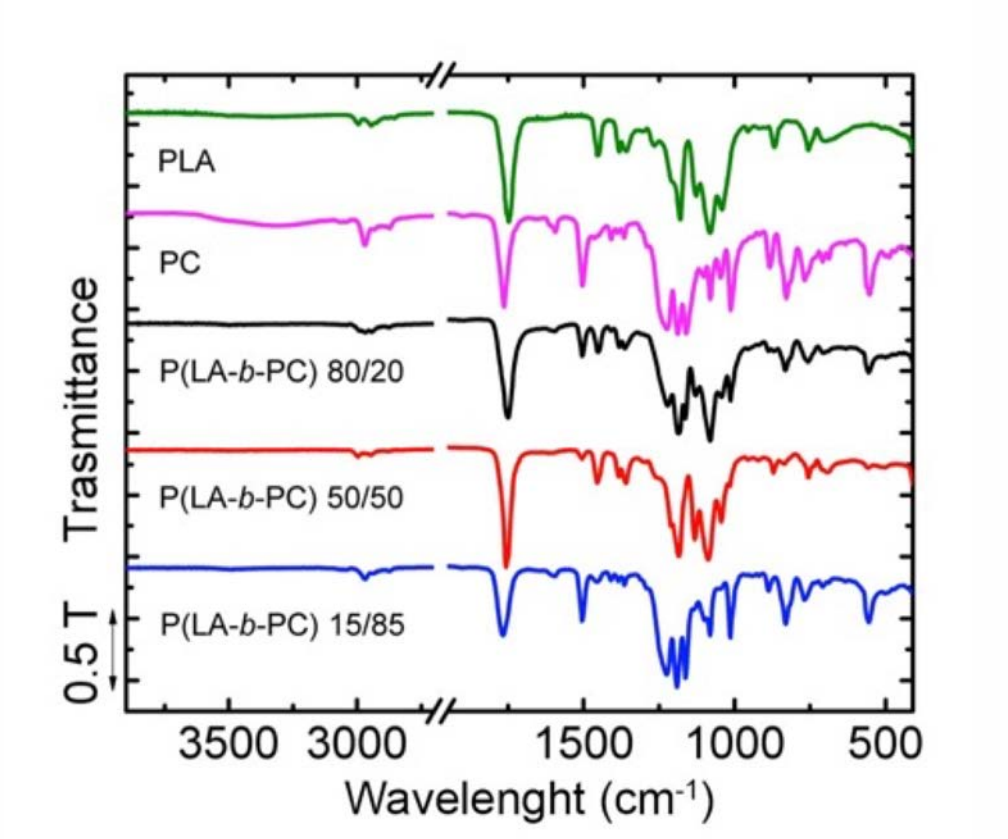

Figure 4.5: ATR spectrum of P(LA-*b*-C) copolymers in compairson with neat PLA and neat PC

as a single peak less intense witch is the same pattern shown in the spectrum of neat PC oligomers.

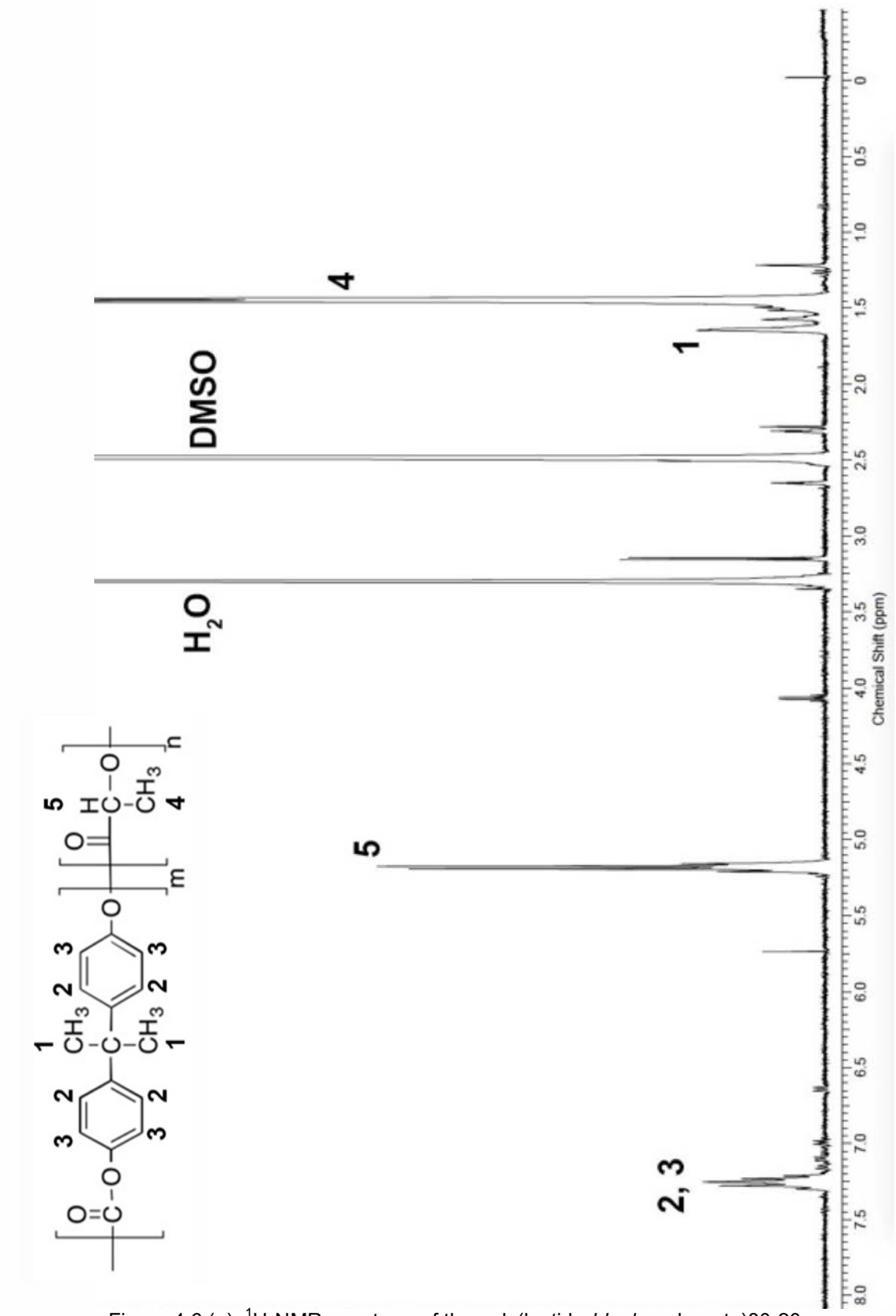

Figure 4.6 (a): ^{1}H-NMR spectrum of the poly(lactide-*block*-carbonate)80-20

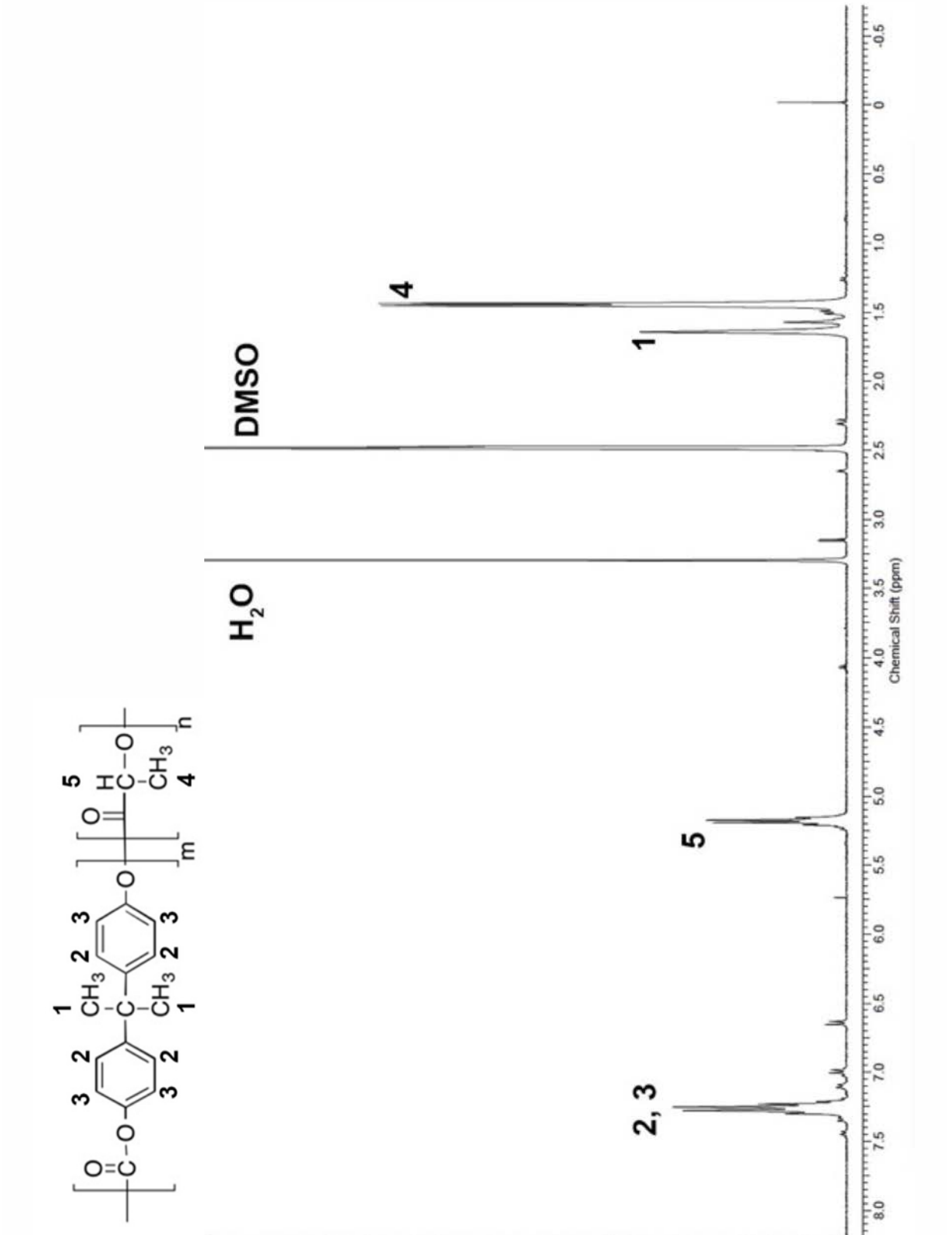

Figure 4.6 (b): ^{1}H-NMR spectrum of the poly(lactide-*block*-carbonate)50-50

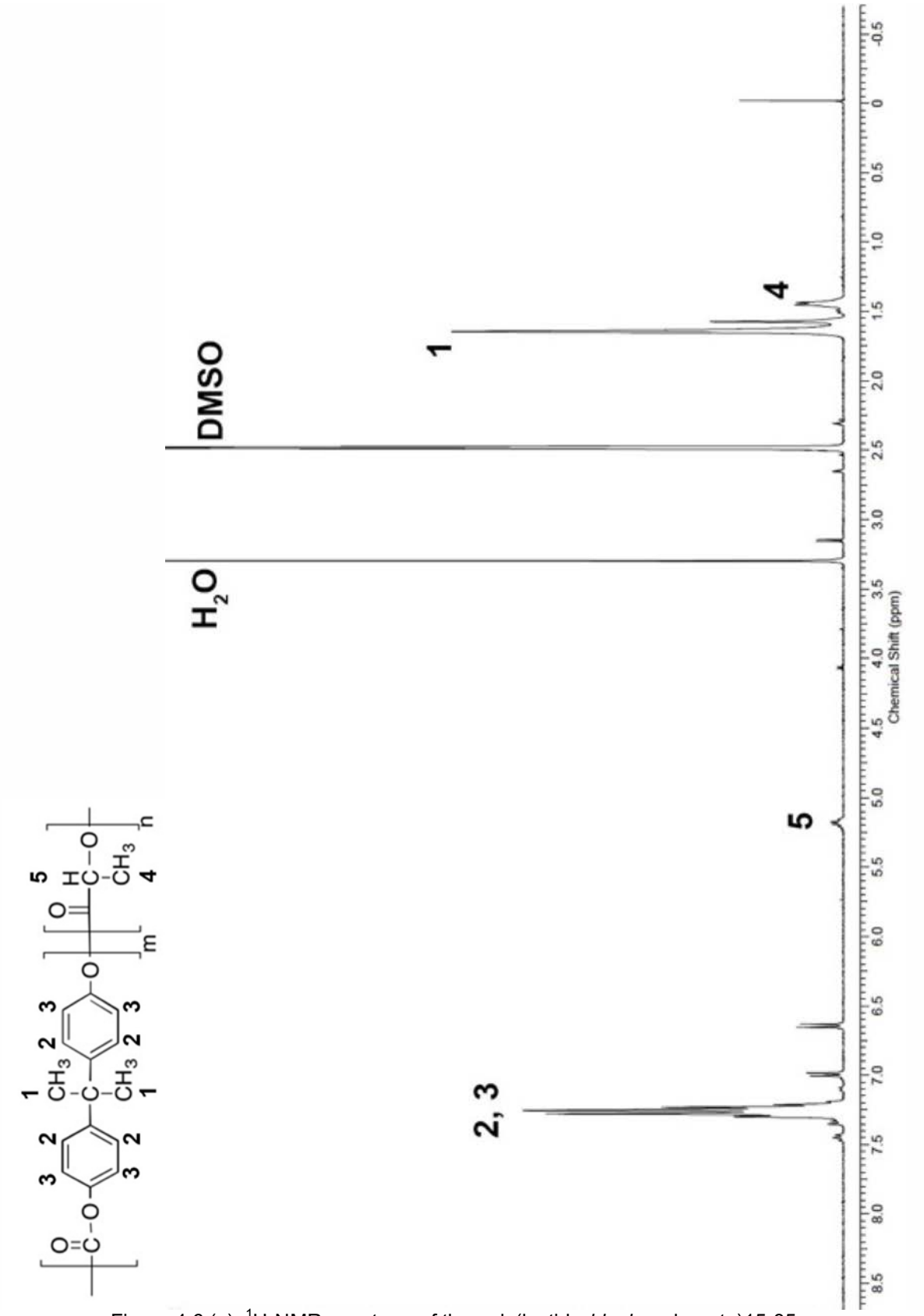

Figure 4.6 (c): ^{1}H-NMR spectrum of the poly(lactide-*block*-carbonate)15-85

4.2 Non-isothermal DSC experiments on P(LA-*b*-C) copolymers

Figure 4.7 shows DSC scans of P(LA-*b*-C) copolymers, used as compatibilizers in PLA/PCL 80/20 blend. In Table 4.2 are reported the Tg values recorded during the scans.

During the first heating scan P(LA-*b*-C)50-50 and P(LA-*b*-C)15-85 show two Tg values, corresponding to PLA and PC blocks. In P(LA-*b*-C)80-20 the Tg of the PC block is overlapped with PLA melting peak (Fig. 4.7a). On the other hand, during the second heating, single glass transition temperatures are visible (Figure 4.7c). These Tg values depend on the composition of the copolymers (Table 3.1) and fit the value predicted by the Fox-Flory equation (11), as shown in Figure 4.8.

$$\frac{1}{Tg} = \frac{w_1}{Tg_1} + \frac{w_2}{Tg_2} \qquad \text{Eq. (11)}$$

Where w_1 and w_2 are the weight fractions of the two components and Tg_1 and Tg_2 the Tg values of the neat homopolymers.

This unusual behaviour depends on the thermal history of the samples. First heating scans reflect a phase segregation behaviour of the two blocks of the copolymers, resulting after the precipitation in methanol (see details of the synthesis in paragraph 3.2). Once the thermal history is erased, at the melt state the two PLA-PC blocks became miscible and, therefore, a single Tg value is visible in the subsequent cooling and heating scans shown in Figure 4.7 (b) and (c).

The behaviour of the copolymers was compared with PLA/PC blends with the same PLA/PC w/w ratio: PLA/PC 80/20, PLA/PC 50/50, PLA/PC 15/85.

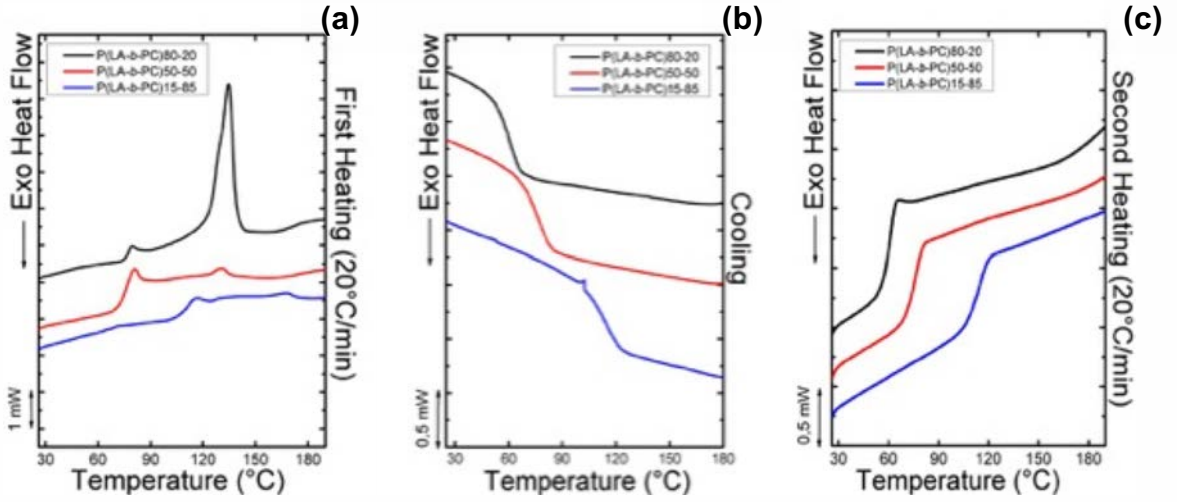

Figure 4.7**:** Non-isothermal DSC experiments on P(LA-*b*-C)s copolymers. (a) First heating curves at 20 °C/min, (b) cooling curves from the melt state, (c) subsequent heating curves at 20 °C/min. The curves have been normalized by the weight of the samples.

Table 4.2: Glass transition temperature (Tg) values for P(LA-*b*-C) copolymers measured during the first heating and second heating DSC scan at 20 °C/min.

Sample	First Heating		Second Heating
P(LA-*b*-C)80-20	78	-	62
P(LA-*b*-C)50-50	76	127	76
P(LA-*b*-C)15-85	112	128	115

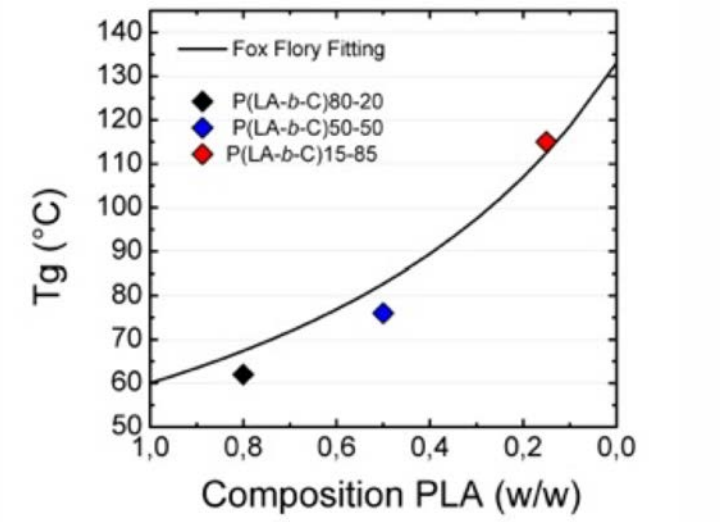

Figure 4.8: Glass transition temperature (Tg) measured during second heating scan, of P(LA-*b*-C) copolymers as a function of the amount of PLA. The solid curve corresponds to the Tg values calculated by applying the Fox-Flory Equation.

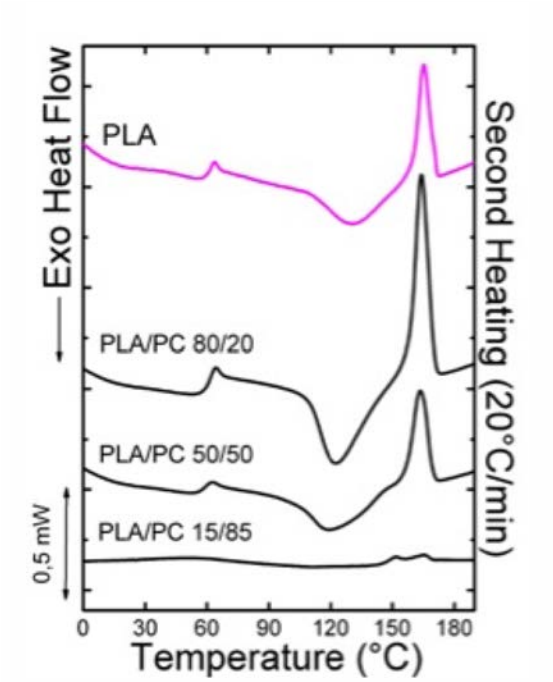

Figure 4.9: DSC experiments on PLA/PC's blend. Second heating curves measured at 20 °C/min

Figure 4.9 shows the second heating curves of PLA/PC blends at 20 °C/min. In all the blends, the Tg of PLA phase does not change in comparison with neat PLA (Tg_{PLA} = 60 °C). The Tg of PC phase, that occurs at 133 °C, isn't observable due to the overlap with the PLA cold crystallization peak, confirming the expected behaviour for this kind of blends [35, 55].

The comparison of the copolymers with PLA/PC blends confirms that the miscibility between the PLA and PC phases could be reached only if the two polymers chains are covalently bonded. Otherwise, also in the second heating of the PLA/PC blends in the same composition a single glass transition temperature should be detected.

4.3 TGA analyses on P(LA-*b*-C) copolymers

Figure 4.10 shows thermograms of the P(LA-*b*-C) copolymers. In each figure, two scans are reported. The first one, denoted with solid line, corresponds to the thermal degradation behaviour of the copolymers without pre-heating. The second one, denoted with dashed lines, corresponds to the thermal degradation behaviour after a pre-heating step from 40 °C to 190 °C at 20 °C/min performed. In any case, the copolymers degrade from 200 °C to 550 °C but if pre-heated they presented a different behaviour. The thermal data obtained are reported in Table 4.3.

In the scans without pre-heating, two degradation steps are visible. The first degradation step starts at 200 °C and it is due to the degradation of PLA block, as reported in literature [56]. The second one starts at 500 °C and, according with literature [57], is referred to the degradation of the PC block. The amount of mass loss for each step reflects the composition of the copolymers and it is characteristic of two immiscible blocks.

In the scans with the pre-heating, a single degradation peak is visible for each copolymer. This degradation peak starts at a temperature intermediate between the two degradation temperatures of PLA and PC blocks, by following the composition of the copolymers. This behaviour is characteristic of two miscible blocks.

Results obtained with TGA characterization are consistent with previous DSC experiments, confirming the miscible-immiscible nature of our copolymers depending on the thermal history. In fact, also in this case, the two blocks exhibit an immiscible behaviour without pre-heating, while after a first heating scan a miscibility behaviour between the PLA and PC blocks is clearly observable. This is because when melted, the two blocks became miscible.

Table 4.3: Data obtained from TGA analysis for (a) P(LA-*b*-C) copolymers and for (b) P(LA-*b*-C) copolymers with a pre-heating step.

(**a**)

P(LA-*b*-C)	T (10%) (°C)	T onset 1 (°C)	T onset 2 (°C)	T peak 1 (°C)	T peak 2 (°C)	Residue %
80-20	218	203	-	252	-	15
50-50	231	224	483	249	496	14
15-85	240	224	484	250	502	18

(**b**)

P(LA-*b*-C)	T (10%) (°C)	T onset 1 (°C)	T onset 2 (°C)	T peak 1 (°C)	T peak 2 (°C)	Residue %
80-20	218	203	-	-	-	17
50-50	232	235	463	250	499	13
15-85	266	236	341	260	497	18

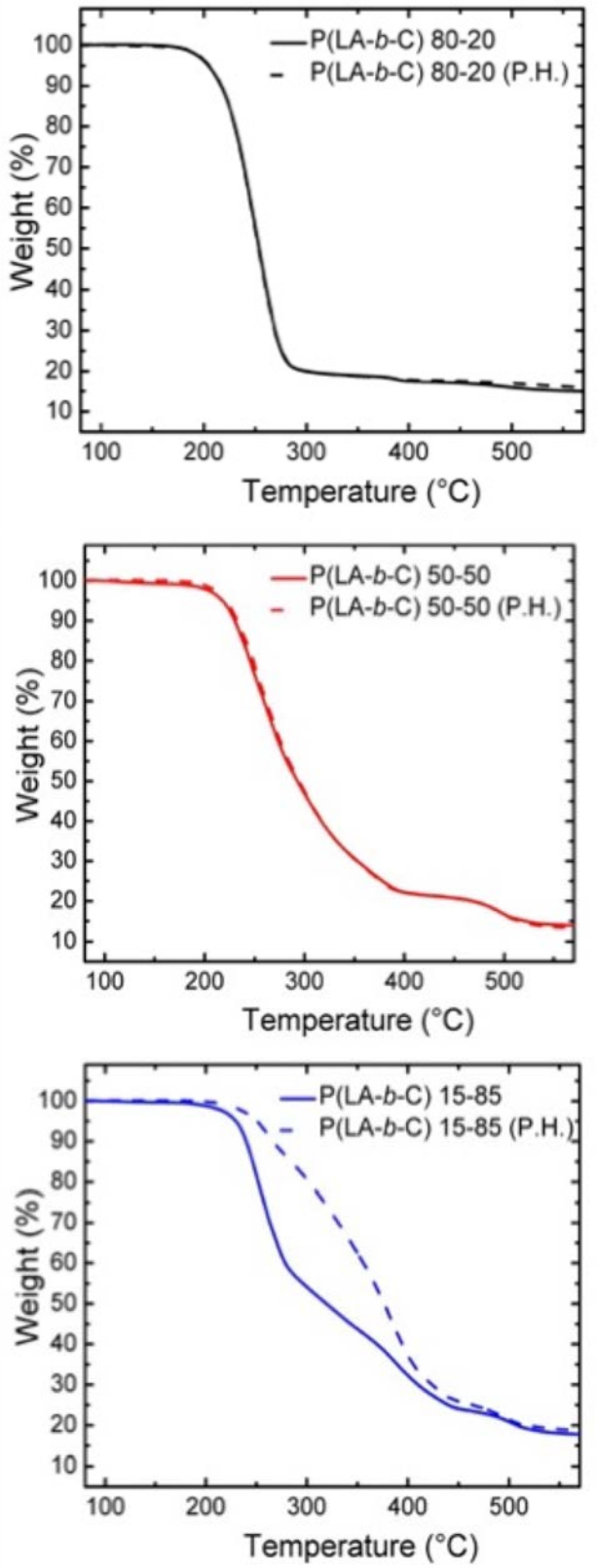

Figure 4.10: TGA curves of P(LA-*b*-C) copolymers. The dashed curves are obtained after a pre-heating (P.H.) of the samples from 40 °C to 190 °C at 20 °C/min.

4.4 SEM micrographs

Figure 4.11 shows SEM micrographs for cryogenically fractured surfaces of PLA/PCL and PLA/PCL/P(LA-*b*-C) blends. In all cases a *sea island morphology*, which is typical of immiscible blends, is observed. This evidence confirms previous works on PLA/PCL 80/20 blends, where the immiscibility of the blend was evidenced [58, 43, 59].

PLA conforms the matrix while PCL is dispersed in droplets. The size of these droplets indicates the degree of compability between PLA and PCL phases [60]. A reduction of the PCL particle size is due to a reduction of the interfacial tension between PLA and PCL and thus to an increase in the compability.

In Table 4.4 PCL droplet diameters, measured by counting at least 100 particles, are reported. In PLA/PCL 80/20, the PCL average particle size (d_n) is 2.48 μm while upon copolymer addition, the PCL particles size is clearly reduced. In particular, upon the addition of P(LA-*b*-C)80-20 and P(LA-*b*-C)50-50, PCL particles size is respectively reduced two and threefold when compared with the blend without copolymers. These results suggest that the block copolymers migrate to the PLA-PCL interphase reducing interfacial tensions between the phases and thus improve dispersion.

On the other hand, neat PC addition does not cause any reduction of the PCL particle size. It basically means that PC does not migrates to the PLA-PCL interphase, but it is dispersed in one or both phases. In fact, Figure 4.11(e) shows two kinds of dispersed phases: the PC domains, present as small spherical droplets (d_n = 1.20 μm) immiscibile with the PLA matrix, and PCL droplets, d_n 2.21 μm. In order to confirm this hypothesis and state the immiscibility between PLA and PC, SEM micrographs of cryogenically fractured surfaces of PLA/PC blends of different compositions are presented in Figure 4.12. In all cases the typical *sea*

Table 4.4: Number average (d_n) and volume average (d_v) particle diameters and particle size distributions (D) and standard deviation (SD) of the PCL phase in PLA/PCL and PLA/PCL/Compatibilizer blends by solvent casting.

Sample	d_n (μm)	d_v (μm)	D	SD
PLA/PCL	2.48	4.34	1.75	0.64
PLA/PCL/P(LA-*b*-C)80-20	1.72	2.12	1.23	0.22
PLA/PCL/P(LA-*b*-C)50-50	0.79	0.91	1.15	0.01
PLA/PCL/P(LA-*b*-C)15-85	2.23	2.94	1.32	0.34
PLA/PCL/PC	2.21	6.42	2.90	0.80

island morphology is revealed, confirming the immiscibility between PLA and PC phases. However in this case no significant variation of the PC particles are detected upon the changes in composition since the differences in the amount of PC in the blend is very low.

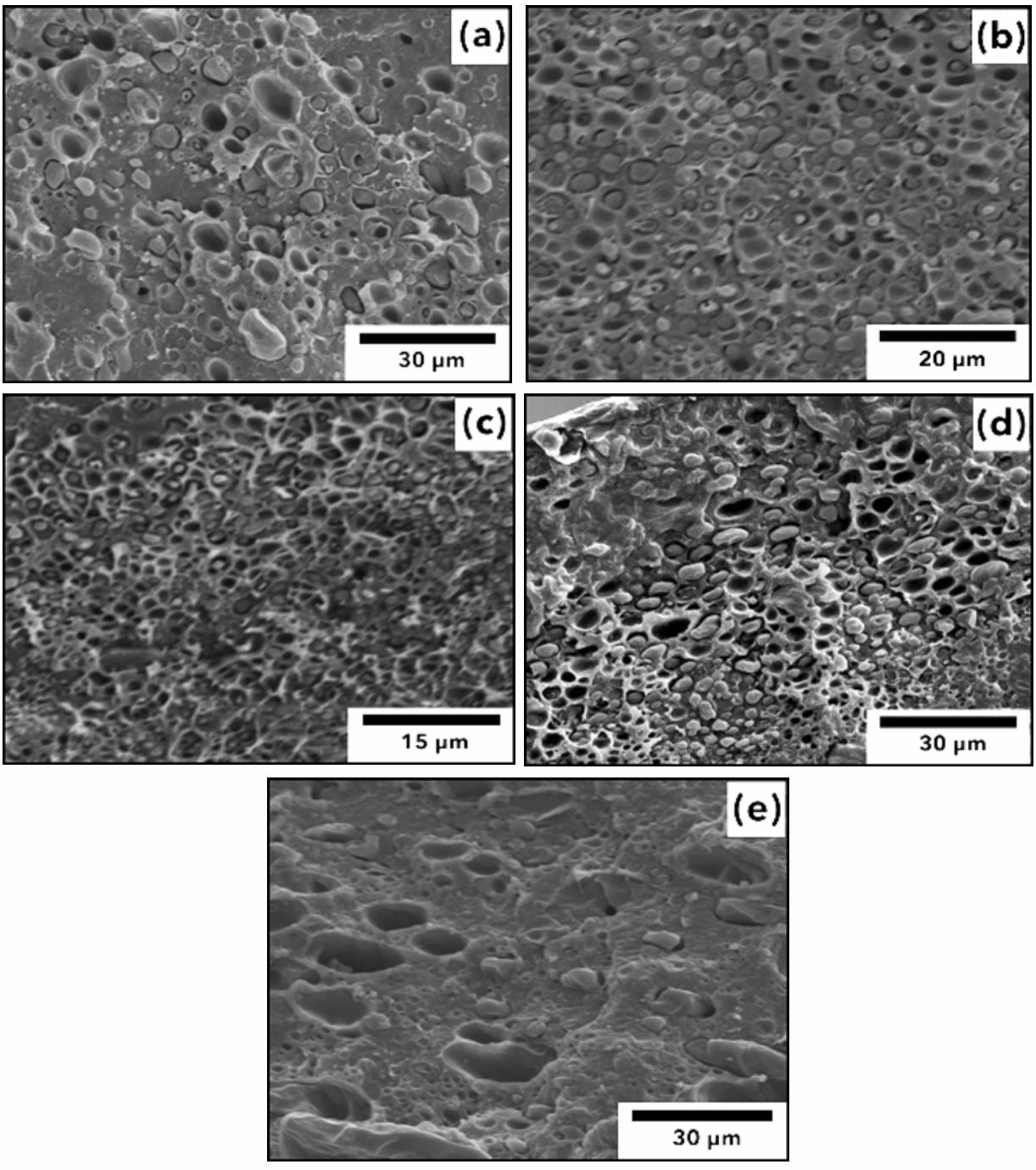

Figure 4.11: SEM micrographs for the cryogenically fractured surfaces of (a) PLA/PCL 80/20 (b) PLA/PCL/P(LA-*b*-C)80-20 (c) PLA/PCL/P(LA-*b*-C)50-50 (d) PLA/PCL/P(LA-*b*-C)15-85 (e) PLA/PCL/PC blends.

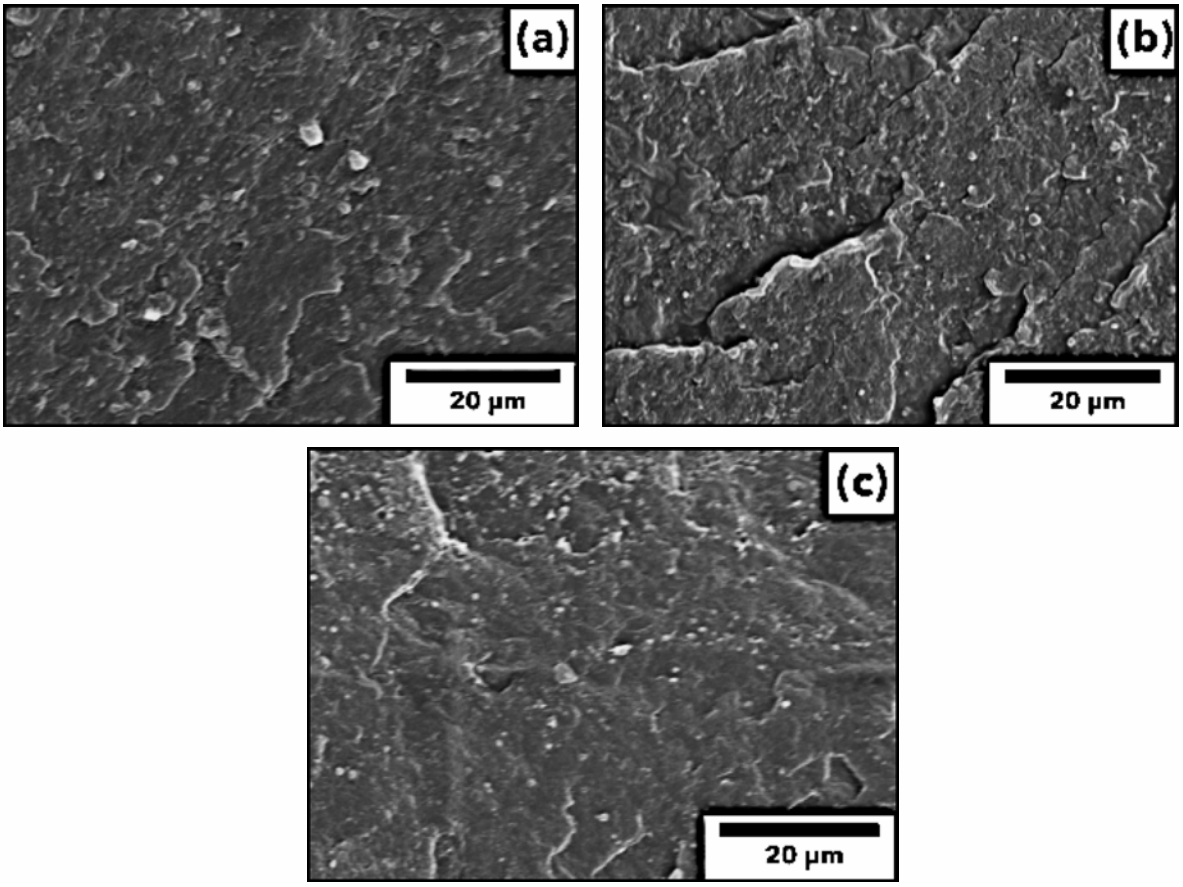

Figure 4.12: SEM micrographs for the cryogenically fractured surfaces of (a) PLA/PC 99/1 (b) PLA/PC 98/2 (c) PLA/PC 95/5 blends.

4.5 Non-isothermal DSC experiments–Cooling from the melt state

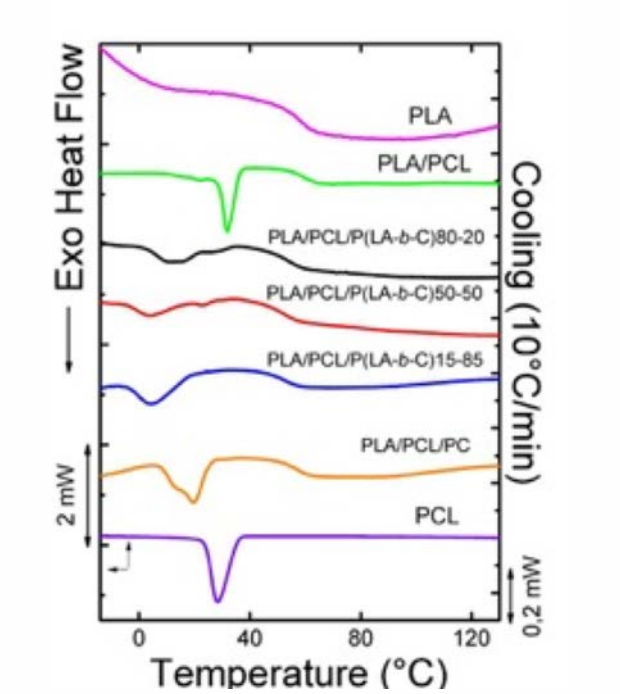

Figure 4.13: Non isothermal DSC experiments. Cooling curve at 10°C/min starting from the melt state. The curves have been normalized by the weight of the samples.

Table 4.5: Thermal properties obtained from non-isothermal DSC cooling at 10 °C/min. The enthalpies of crystallization and melting have been normalized by the weight fraction of the samples.

Sample	Comp. (w/w)	PCL		PLA		
		Tc (°C)	ΔHc (J/g)	Tg (°C)	Tc (°C)	ΔHc (J/g)
PLA	100	-	-	59.4	-	-
PLA/PCL	80/20	21.7/31.8	2.6/45	58.2	-	-
PLA/PCL/P(LA-*b*-C)80-20	80/20/2	11/26.9	28.7/4.8	52.7	-	-
PLA/PCL/P(LA-*b*-C)50-50	80/20/2	4.6/23.1	23.5/3.9	48.3	119.2	3.1
PLA/PCL/P(LA-*b*-C)15-85	80/20/2	5	35.4	51.9	93.1	1.8
PLA/PCL/PC	80/20/2	12/19.7	15.3/33.5	57.5	93.1	1.7
PCL	100	28.8	57.2	-		-

Figure 4.13 shows cooling DSC scans at 10°C/min from the melt state for blends and neat components. Table 4.5 reports the values of the thermal transitions recorded during cooling.

Neat PCL crystallizes during cooling at 29 °C with a sharp exothermic peak. However, when PCL is dispersed in the PLA matrix it exhibits the characteristic fractionated crystallization peak. Fractionated crystallization is a common

occurrence in immiscible blends. It happens when the number of droplets of a crystallizable phase is larger or of the same order of magnitude as the number of active heterogeneities present in the bulk polymer before being dispersed [50,61,62,63].

As shown in Table 4.5, PCL droplets dispersed in PLA/PCL crystallizes in two peaks at 21.7°C and 31.8 °C. The peak at 31.8°C is related to a PCL population nucleated by more active heterogeneities (lower supercooling) while the peak at 21.7 °C is referred to PCL droplets nucleated by less active heterogeneities. Upon the P(LA-*b*-C) copolymers addition, PCL crystallization peaks are shifted to lower temperatures. In these cases PCL droplets are smaller than in neat PLA/PCL blend (according to Table 4.4) therefore the probability to find active heterogeneities is reduced and the droplets need a higher supercooling to crystalize.

Neat PLA does not exhibit any crystallization peak during cooling at the rate employed (10 °C/min) since it contains a significant amount of D-Lactide (PLA used 4032D: 1.2-1.6% of D-Lactide) that interrupts L-lactide crystallisable sequences and together with the high Mn value induces a slow crystallization rate [64]. The same behaviour is detected for PLA/PCL since, being immiscible, the PLA phase crystallization is not affected by the presence of PCL.

On the other hand, when the block copolymers are added to the blend, a small crystallization peak corresponding to PLA phase is detected. It confirms that the copolymers increase the miscibility between PLA and PCL phases, promoting the plasticization of PLA by PCL chains (as PCL is a very flexible polymer characterized by a Tg of approximately −60 °C). In particular, the blend that presents the lowest PCL particle size (PLA/PCL/P(LA-*b*-C)50-50 according to Table 4.4) presents the highest PLA block crystallization enthalpy.

Another confirmation of the compatibilizer effect of the block copolymer is detectable by looking at the Tg values of the PLA phase (Table 4.5). Polymer blends that are completely immiscible exhibit two separated Tg values corresponding to those of the pure components. When the components of the blends are miscible, a single Tg is observed at intermediates values (according to the Fox-Flory equation (11)) [65]. Partial miscibility, on the other hand, is characterized by the presence of two Tg transitions located at values that are different from those of the neat components and shifted towards one another.

Therefore, since Tg of PLA is 60°C and the Tg of PCL is -60°C, in case of improved miscibility a decrease of the Tg of the PLA phase is expected.

According to Table 4.5, neat PLA exhibits a glass transition temperature of 59.4 °C. Blending with PCL does not cause a significant variation (i.e. Tg of PLA in PLA/PCL it's 58.2°C) while upon the addiction of P(LA-*b*-C)s copolymers a decrease is detected. This reduction agrees with the previous results, since the blend that shows the greatest reduction of Tg (PLA/PCL/P(LA-*b*-C)50-50 Tg=48.3°C) shows the largest PCL droplet size reduction and PLA crystallization peaks.

In order to confirm these results, an analysis of the isothermal spherulitic growth rate of the PLA phase in the blend was performed.

4.6 Spherulitic growth rate of PLA from the melt state

In all prepared samples, PLA spherulites grow linearly with time, indicating that no diffusion problems at the growth front are induced by blending. The spherulitic growth rate G (μm min^{-1}) was thus calculated from the slope of the line obtained from the spherulitic radius (μm) against time (min). Figure 4.14 shows G values at different crystallization temperatures fitted by an arbitrary function to guide the eye.

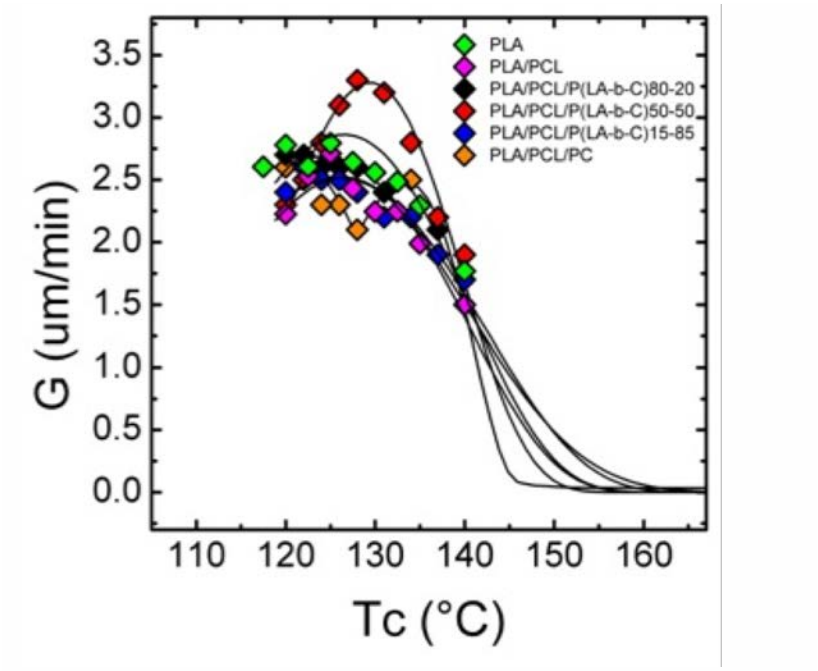

Figure 4.14: Spherulitic growth rate G as a function of isothermal crystallization temperature T_c for neat PLA and PLA phase within PLA/PCL and PLA/PCL/Compatibilizer blends. The solid lines represent arbitrary fits to guide the eye.

It is possible to observe that all the samples exhibit the well-known bell-shaped trend due to the dependence of the spherulites growth rate (G) with the crystallization temperature [66]. Such dependence evidences that secondary nucleation dominates the right hand side of the bell shape curve, while below a critical temperature diffusion takes over and the growth rate decreases as the Tc values approach Tg.

At temperatures lower than 120°C, it is not possible to collect any data since the nucleation rate is too high and the spherulites immediately collide.

Figure 4.14 shows that values of spherulitic grow rate obtained for the PLA phase within PLA/PCL blends are close to those obtained for neat PLA. This result confirms the immiscibility of PLA with PCL. Otherwise a change in spherulitic growth kinetics of PLA would be detected, as any amount of dissolved PCL chains within a PLA-rich phase would enhance molecular diffusion.

On the other hand, when P(LA-*b*-C)50-50 is added to the blend an enhancement of the PLA spherulitic growth rate is observable. At a temperature of 130°C, the G value in PLA/PCL/P(LA-*b*-C)50-50 is 3.25 μm min^{-1} while in neat PLA is 2.50 μm min^{-1}. This is another evidence indicating that P(LA-*b*-C)50-50 is a compatibilizer agent for PLA/PCL 80/20 blends.

4.7 Spherulitic Morphology

PLOM micrographs in Figure 4.15 shows the PLA spherulitic morphology of neat PLA and of PLA phase within the blend at the same temperature of crystallization (126 °C) and at the same crystallization time (5 minutes after the beginning of the PLA crystallization).

PLA spherulites shows the typical Maltese cross morphology with a negative sign [64]. In PLA/PCL 80/20 blend (Fig. 4.15b) small PCL droplets can be observed in the melt surrounding the spherulites, indicating that there are two immiscible phases. In all the compatibilized blends (Fig. 4.15c, 4.15d, 4.15e, 4.15f) PCL droplets can be observed both in the melt surrounding the spherulites and inside the spherulites (as black dot) confirming that a certain degree of compatibility is achieved during blending. In PLA/PCL/PC blend (Fig. 4.15f) two droplets populations with different sizes can be observed in the melt surrounding

the PLA spherulites. This is due, according with SEM micrographs, to the presence of both PCL and PC as dispersed phases.

Comparing the images presented in Fig. 4.15, it can be observed that PLA spherulites in PLA/PCL/P(LA-*b*-C)50-50 blend (Fig. 4.15d) exhibit larger radii in comparison with those of other PLA/PCL/Compatibilizer blends. This result is consistent with the increase of PLA spherulitic growth shown in the previous paragraph (Figure 4.14).

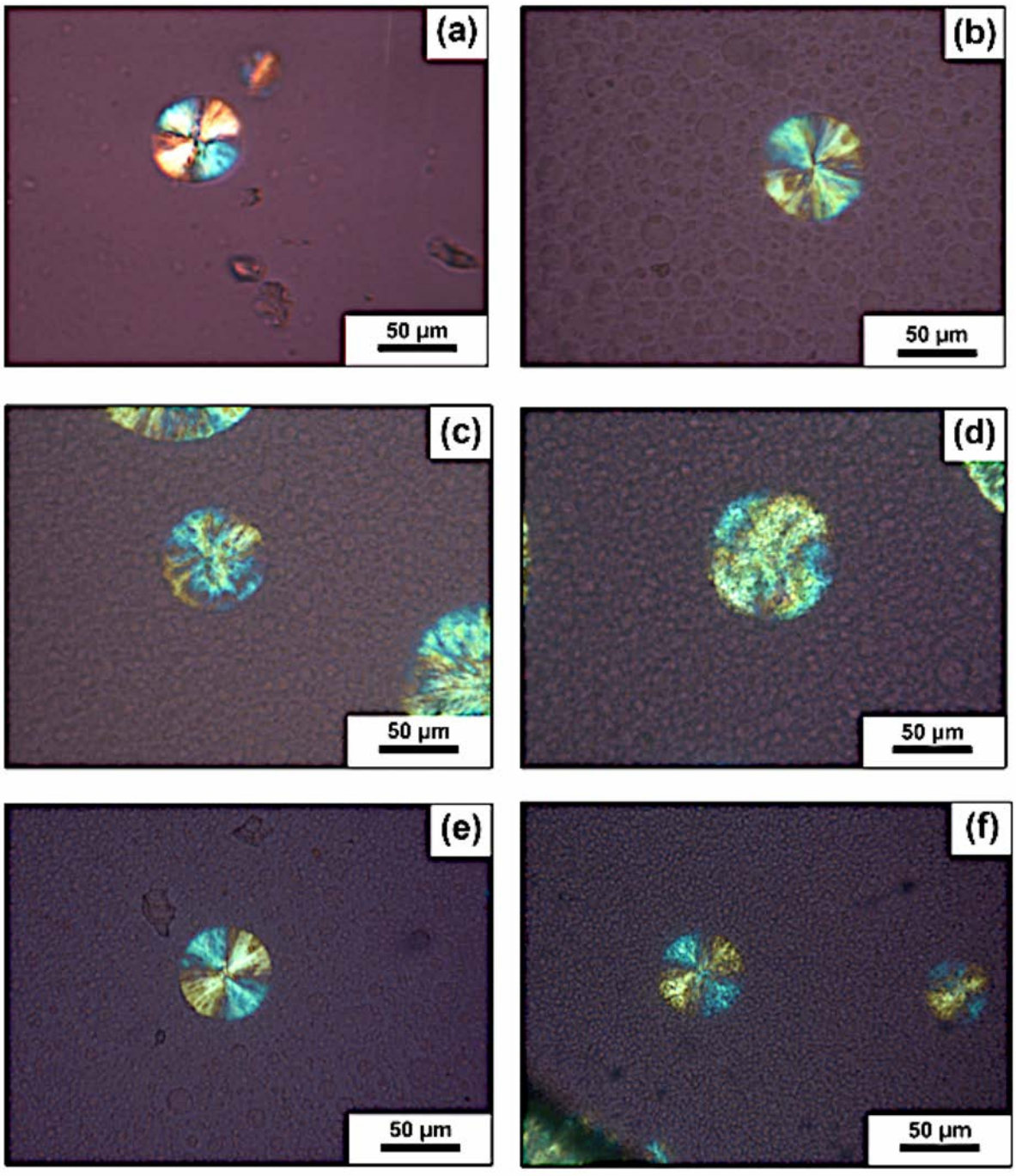

Figure 4.15: PLOM micrographs of (a) PLA (b) PLA/PCL (c) PLA(PCL/P(LA-*b*-C)80-20 (d) PLA/PCL/P(LA-*b*-C)50-50 (e) PLA/PCL/P(LA-*b*-C)15-85 (f) PLA/PCL/PC recorded at 128 °C and after 5 minutes from the begin of the crystallization.

4.8 Combined Isothermal/Non-Isothermal DSC Experiments on PCL

In order to investigate the compatibilization ability of the copolymers, attempts were made to determine the isothermal crystallization rate of the PCL phase within the blends. However, the crystallization rate of PCL is so fast that it crystallizes upon cooling from the melt in the DSC even when cooling rates of 60°C/min are employed. To overcome these difficulties, a combined isothermal/non-isothermal experiments was designed. The samples were first heated to 200 °C and kept at that temperature for 3 minutes to erase the thermal history. Then they were cooled at 60°C/min (in order to avoid PLA crystallization during cooling) until specific isothermal crystallization temperatures between 54 °C and 0 °C and held at this temperature for 15 minutes. Then the samples were reheated at 20 °C/min to 200 °C.

Fig. 4.16 shows the data obtained by isothermal/non-isothermal experiments where the PCL heat of fusion is plotted as a function of the isothermal crystallization temperature. Data obtained shows that neat PCL exhibits a lack of dependence of the melting enthalpy from the isothermal crystallization temperature. This means that PCL crystallization is not affected by the isothermal crystallization step and, thus, neat PCL crystallizes during the previous non-isothermal cooling. Fig. 4.16 shows that blending PCL with PLA, the PCL enthalpy of melting decreases with increases in the T_c. According to Table 4.4, this behaviour is due to the confinement of PCL droplets into the PLA matrix that, as reported in literature [67], cause a reduction of the PCL crystallization temperature during the cooling and therefore, it needs more supercooling to crystallize. The enthalpy of melting of PCL phase within the PLA/PCL 80/20 blend starts to decrease from Tc values larger than 35 °C. This means that in this blend PCL reaches its maximum rate of crystallization at temperatures below 35 °C while for neat PCL the maximum has been already reached at 45 °C.

Fig. 4.16 also shows that upon the P(LA-*b*-C)s addiction, the decrease of the PCL heat of fusion with Tc is larger. This is related to the compatibilizer effects of the copolymers that, as shown by the SEM micrographs and non-isothermal DSC results, promote a further confinement of PCL droplets within the PLA matrix and thus a reduction of PCL crystallization temperature. The blend that shows the

highest reduction of PCL heat of fusion is the PLA/PCL/P(LA-*b*-C)50-50. This result is in accord with what was previously asserted: the P(LA-*b*-C)50-50 copolymer shows the highest enhancement of miscibility among PLA/PCL/Compatibilizer 80/20/2 blends, giving the highest reduction of PCL average particle size (as shown in Table 4.4). For the PLA/PCL/P(LA-*b*-C)15-85 blend, the PCL particle average size is almost the same in comparison with the blend without compatibilizer. However, the PCL heat of fusion also decreases with Tc. It is speculated that this behaviour is related to the copolymer addition which, according to the literature [68], inhibits the PCL phase crystallization.

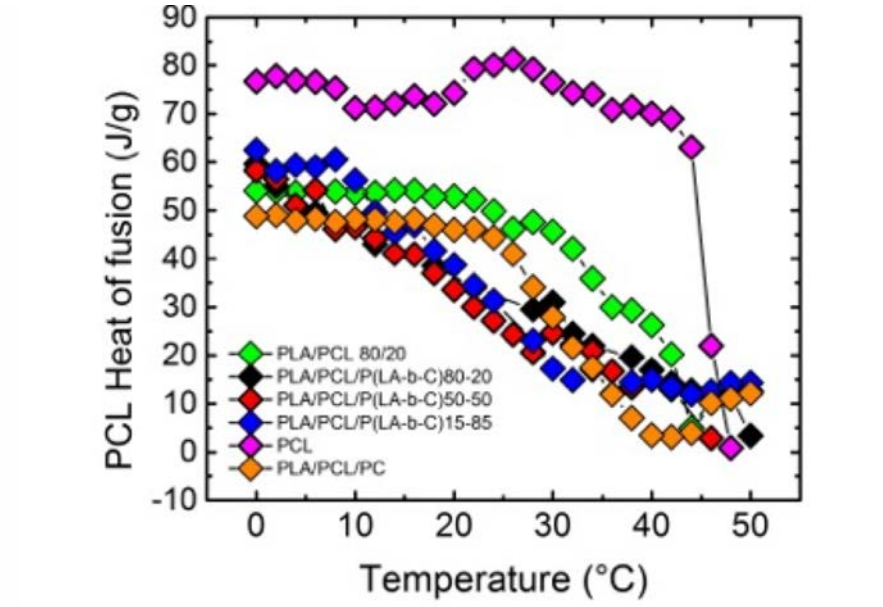

Figure 4.16: Combined non-isothermal/isothermal DSC experiments. PCL heat of fusion recorded during second heating as a function of the isothermal crystallization temperature (Tc)

4.9 Non-isothermal DSC experiments – Second Heating

Figure 4.17 shows second heating curves corresponding to non-isothermal DSC experiments at 10°C/min, while in Table 4.6 the thermal transition values derived from these traces are reported.

Neat PLA and PLA phase within the blends exhibits cold crystallization peaks between 130°C and 100°C. Although PLA is not able to crystallize during cooling from the melt at the scanning rate employed (10 °C/min), it can crystallize during subsequent heating at the same rate. This effect is due to the cooling at temperature below Tg (Tg PLA: 60°C, Cooling scan: from 200°C to -20°C) that

causes the formation of active nuclei in PLA, promoting the crystallization in the subsequent heating scan [69].

The cold crystallization behaviour of PLA is also influenced by the presence of PCL. While neat PLA shows a broad exothermal peak around 130°C, by blending with PCL the cold crystallization peak appears sharper and its position is decreased to 110°C. This indicates that PCL nucleates the cold crystallization of PLA.

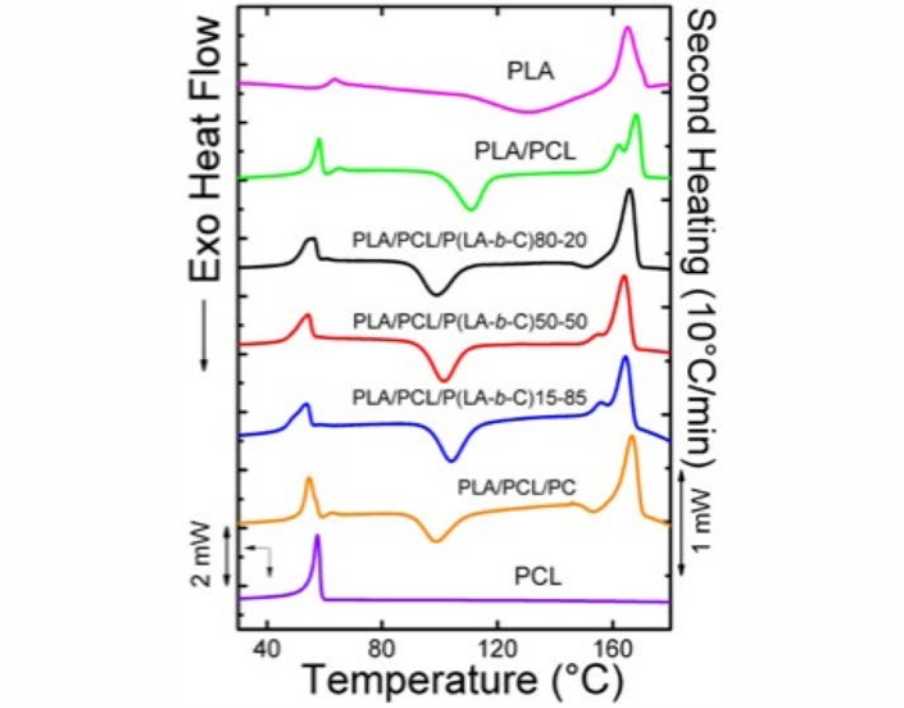

Figure 4.17: Non isothermal DSC experiments. Second heating curves of neat PLA and PCL, PLA/PCL, PLA/PCL/Compatibilizer at 10°C/min. The curves have been normalized by the weight of the samples

Table 4.6: Thermal properties obtained from non-isothermal DSC heating at 10 °C/min. The enthalpies of crystallization and melting have been normalized by the weight fraction of the samples.

	Comp. (w/w)	PCL		PLA			
		Tm (°C)	ΔHm (J/g)	Tcc (°C)	ΔHcc (J/g)	Tm (°C)	ΔHm (J/g)
PLA	100	-	-	129.1	27.8	165.6	33.3
PLA/PCL	80/20	58.2	49	110.8	27.9	162.4/167.8	15.6/16.6
PLA/PCL/P(LA-*b*-C)80-20	80/20/2	56	39.1	98.9	27.5	165.9	35.9
PLA/PCL/P(LA-*b*-C)50-50	80/20/2	54.4	38.7	101.5	28.9	155/164	4.4/30.8
PLA/PCL/P(LA-*b*-C)15-85	80/20/2	53.9	47.8	103.9	29.2	156/164	6.1/26.9
PLA/PCL/PC	80/20/2	54.7	47.3	98.7	24	166.7	36.1
PCL	100	57.8	63.2	-	-	-	-

Upon addition of the block copolymers or PC the cold crystallization of PLA is even more enhanced. This indicates that the blending of both compatibilizers could further facilitate the formation of active nuclei in PLA. However, only by non-isothermal analysis is not possible to understand the mechanism that allow this effect. So, an isothermal analysis on PLA crystallization from the glassy state was performed.

4.10 Isothermal DSC experiments of PLA from the glassy state

Previous results demonstrated that the enhancement of PLA cold crystallization in the PLA/PCLs blends is consistent with an acceleration of PLA nucleation, since no significant variation of PLA spherulities growth rate upon blending with PCL is detected. Therefore, the nucleation behaviour after cooling below Tg was investigated by an Isothermal DSC experiments.

Figure 4.18 shows the inverse of half-crystallization time as a function of crystallization temperature for neat PLA and for the blends. The inverse of the half-crystallization time (defined as the time required to attain half of the final crystallinity) at a given temperature indicates the overall crystallization rate. The black lines correspond to arbitrary fits performed to guide the eye.

Data obtained shows that all the samples display the typical *bell-shape* trend, where the crystallization rate goes trough a maximum as the kinetics changes from nucleation control at higher temperatures to a diffusion control at lower temperatures [10].

The overall crystallization rate of a semi-crystalline polymer is mainly governed by nucleation and growth rate of the crystals. Since PLA spherulitic growth rate is not sensitive to blending, the differences between the data in Figure 4.18 are due to differences in nucleation rate.

The values in Figure 4.18 are observed to follow the enhancement of cold crystallization noted by non-isothermal analysis.

According to Figure 4.18, neat PLA completes its crystallization at the maximum (T_c=120 °C) in 8 minutes. Taking PLA as reference material, an enhancement effect on nucleation rate is clearly evident by blending with PCL. In PLA/PCL, the PLA phase completes its crystallization at the maximum (T_c=120 °C) in 1.5 minutes, while in PLA/PCL/PC and PLA/PCL/P(LA-*b*-C)80-20, a further effect on the crystallization is detected. In PLA/PCL/P(LA-*b*-C)80-20 the PLA phase

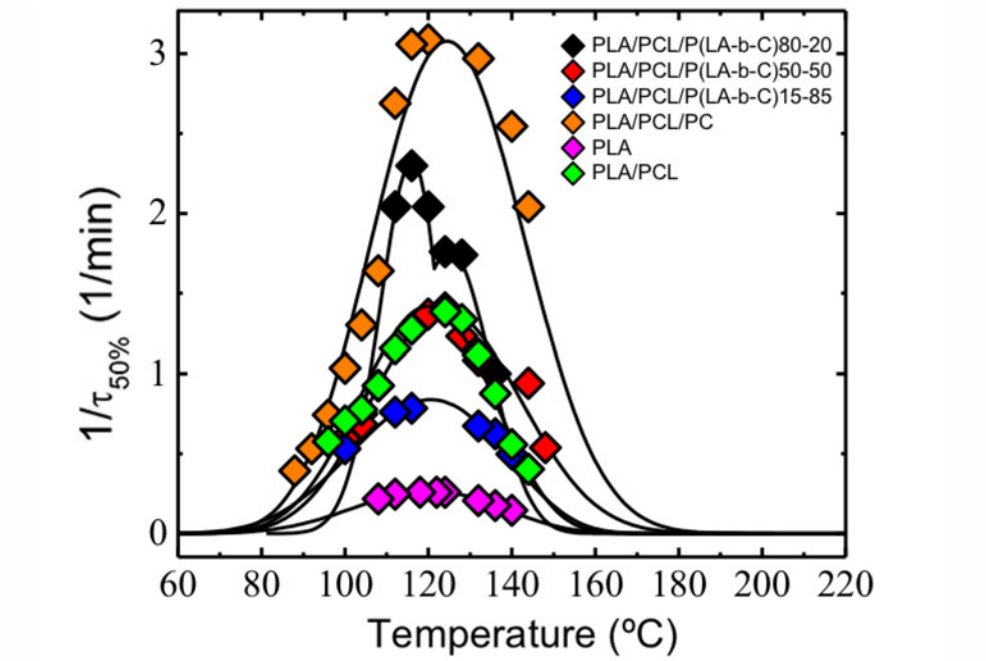

Figure 4.18: Isothermal crystallization experiments conduced from the glassy state. Overall crystallization rate ($1/t_{50\%}$) as a function of isothermal crystallization temperature T_c in neat PLA and PLA phase within PLA/PCL and PLA/PCL/Compatibilizer blends. The solid lines rapresent arbitrary fits to guide the eye.

crystallizes at 116°C, ten times faster than neat PLA, while in PLA/PCL/PC at 120 °C the crystallization rate of the PLA phase is even fifteen times higher than neat PLA. On the other hand, the addition of P(LA-*b*-C)15-85 gives rise to a reduction of the crystallization rate in comparison with the values obtained at the same amount of PCL.

The data obtained by isothermal Differential Scanning Calorimetry (DSC) tests were used to perform the Avrami Fits and the graphical comparisons between the experimental data and the predictions of the theory (Figure 4.19). Firstly, it allows the baseline to be established and later calculate the integral of the calorimetric isothermal curve. Secondly, the linear fit according to the Avrami equation and fitting errors can be performed. V_c (relative volume fraction crystallinity) is calculated according to Eq. 12, whereas V_c range is selected from 0.03 to 0.20 in order to obtain the best fit within the primary crystallization range.

$$Vc = \frac{Wc}{Wc + \frac{\rho_c}{\rho_a}(1 - Wc)} \qquad \text{Eq. (12)}$$

Where ρ_c and ρ_a are the fully crystalline and fully amorphous polymer densities, respectively. For all calculations, ρ_a=1.25 g/cm^3 and ρ_c=1.359 g/cm^3 were used for PLA. The relative crystalline mass fraction W_c is calculated as:

$$Wc = \frac{\Delta H_{(t)}}{\Delta H_{TOT}} \qquad \text{Eq. (13)}$$

Where $\Delta H(t)$ and ΔH_{total} are the enthalpy as a function of crystallization time and the maximum enthalpy after completion of the crystallization process.

Finally, the Avrami equation is rearranged as follows:

$$\log[-\ln[1 - V_c(t - t_0)]] = \log(K) + n\log(t - t_0) \qquad \text{Eq. (14)}$$

Where *n* is the Avrami index and *K* is the overall crystallization rate constant. The experimental and predicted half–crystallization $\tau_{50\%}$ can be also determined by this Origin® plugin [70]. According to the Avrami equation, $\tau_{50\%}$ is:

$$\tau_{50\%} = \left[-\frac{\ln[1 - V_c]}{K}\right]^{1/n} \qquad \text{Eq. (15)}$$

Then, depending on the goodness of the fit (up to 50% conversion) there may be a difference between the experimental and predicted values of $\tau_{50\%}$. The parameters obtained by Avrami Fits are collected in Table 4.7.

Table 4.7 shows that the Avrami index values (*n*) for the isothermal crystallization of PLA or the PLA phase within all prepared blends oscillated between 1.5 and 3, it means that crystals have 2-3 dimensions, axialities or spherulities.

In the blend with the lower crystallization rate (neat PLA and PLA/PCL/P(LA-*b*-C)15-85) the value of n is always among 2, that means sporadic nucleation. On the other hand, blends with higher crystallization rate show a decrease in n value from 2 to 1 as T_c increases. This is a typical trend, since nucleation becomes more instantaneous as the temperature increase. [6].

The Avrami index values (*n*) obtained for PLA/PCs blends oscillated between 1 and 2.5 (although in some isolated cases values closer to 3 were obtained). It means that crystals have 2-3 dimensions, axialities or spherulities.

Data obtained shows that most of values of Avrami index are closed to 2. Generally, such a low *n* value is a not so usual in polymeric materials. The reason of this behaviour is related to the high nucleation rate that avoid the evolution of the crystals in a 3D dimension (spherulite).

Table 4.7: Data obtained by the Avrami model

PLA/PCL					
T(°C)	R2	K	n	τ_{THEO} (min)	τ_{EXP} (min)
144	0,9999	0,185	1,3	2,759	2,482
140	1,0000	0,282	1,33	1,965	1,797
136	0,9999	0,579	1,39	1,139	1,140
132	1,0000	0,772	1,49	0,930	0,896
128	0,9999	1,040	1,58	0,776	0,749
124	1,0000	1,100	1,64	0,753	0,722
120	0,9998	1,080	1,81	0,785	0,763
116	0,9997	1,050	1,94	0,807	0,784
112	0,9997	0,891	2,13	0,889	0,865
108	0,9993	0,524	2,37	1,125	1,080
104	0,9991	0,310	2,64	1,355	1,290
100	1,0000	0,308	2,26	1,432	1,419
96	1,0000	0,208	2,14	1,755	1,735

PLA					
T(°C)	R2	K	n	τ_{THEO} (min)	τ_{EXP} (min)
140	0,9996	0,003	2,76	7,023	6,875
136	0,9999	0,007	2,63	5,811	5,703
132	1,0000	0,018	2,31	4,882	4,845
128	0,9997	0,020	2,31	4,686	4,542
124	1,0000	0,033	2,23	3,923	3,867
122	1,0000	0,027	2,35	3,870	3,872
120	0,9994	0,024	2,32	4,273	4,002
116	0,9992	0,024	2,29	4,317	4,025
118	1,0000	0,030	2,26	4,008	3,872
112	0,9998	0,029	2,19	4,255	4,050
108	1,0000	0,027	2,1	4,716	4,604
104	0,9978	0,273	2,43	1,468	1,346
100	1,0000	0,033	2,03	4,462	4,368

PLA/PCL/P(LA-*b*-C)80-20					
T(°C)	R2	K	n	τ_{THEO} (min)	τ_{EXP} (min)
148	0,9984	0,864	1,31	0,845	0,975
144	0,9986	1,170	1,38	0,682	0,787
140	0,9986	0,653	1,3	1,047	1,174
136	0,9989	0,789	1,35	0,909	1,000
132	0,9994	0,878	1,4	0,844	0,893
128	0,9996	1,790	1,56	0,545	0,575
124	0,9999	1,780	1,62	0,559	0,568
120	0,9996	2,830	1,69	0,436	0,490
116	1,0000	3,180	1,81	0,430	0,435
112	0,9999	2,660	1,94	0,500	0,490
108	0,9998	0,767	1,95	0,949	1,082
104	0,9996	0,473	2,14	1,196	1,338
100	0,9996	0,273	2,09	1,561	1,508
96	0,9985	0,260	2,4	1,503	1,458
92	0,9999	0,174	2,76	1,648	1,657
88	0,9999	0,141	2,4	1,944	1,941
84	0,9999	0,076	2,29	2,633	2,607
80	1,0000	0,049	2,07	3,604	3,575

PLA/PCL/P(LA-*b*-C)50-50					
T(°C)	R2	K	n	τ_{THEO} (min)	τ_{EXP} (min)
148	0,9997	0,255	1,36	2,087	1,860
144	0,9995	0,650	1,35	1,049	1,063
140	0,9993	1,330	1,46	0,642	0,685
136	0,9992	2,300	1,59	0,469	0,517
132	0,9999	0,705	1,6	0,990	0,923
128	0,9999	0,890	1,64	0,856	0,812
124	0,9999	1,150	1,71	0,744	0,710
120	0,9995	1,150	1,93	0,771	0,730
116	0,9996	1,320	2	0,725	0,695
112	0,9996	1,330	2,07	0,729	0,707
108	1,0000	0,340	2,19	1,386	1,398
104	1,0000	0,318	2,11	0,446	1,457
100	1,0000	0,240	2,12	1,649	1,680
96	1,0000	0,346	2,41	1,335	1,33
92	1,0000	0,226	2,39	1,598	1,585
88	1,0000	0,076	2	3,034	3,1

PLA/PCL/P(LA-*b*-C)15-85					
T(°C)	R2	K	n	τ_{THEO} (min)	τ_{EXP} (min)
144	1,0000	0,070	1,94	3,272	3,215
140	1,0000	0,103	1,93	2,696	2,726
136	0,9994	0,107	2,2	2,337	2,144
132	1,0000	0,227	2,23	1,651	1,707
128	1,0000	0,396	2,13	1,301	1,349
124	1,0000	0,371	2,16	1,336	1,415
120	0,9999	0,181	2,11	1,890	1,922
116	1,0000	0,184	2,18	1,838	1,912
112	1,0000	0,183	2,13	1,871	1,933
108	1,0000	0,158	2,29	1,906	1,965
104	1,0000	0,194	2,11	1,830	1,862
100	1,0000	0,171	2,07	1,963	1,993
96	1,0000	0,058	2,09	3,283	3,334
92	1,0000	0,086	1,93	2,959	2,893

PLA/PCL/PC					
T(°C)	R2	K	n	τ_{THEO} (min)	τ_{EXP} (min)
144	0,9950	1,450	1,1	0,513	0,490
140	0,9961	2,560	1,22	0,343	0,393
136	0,9958	7,410	1,46	0,197	0,240
132	0,9988	2,320	1,3	0,393	0,337
120	1,0000	5,110	1,8	0,330	0,324
116	0,9999	5,350	1,89	0,339	0,327
112	0,9997	4,470	2,01	0,396	0,372
108	0,9992	1,760	2,21	0,656	0,610
104	0,9989	1,040	2,25	0,836	0,768
100	0,9990	0,635	2,33	1,038	0,967
96	0,9989	0,281	2,48	1,439	1,347
92	0,9992	0,11	2,67	1,992	1,882
88	0,9998	0,061	2,48	2,654	2,554

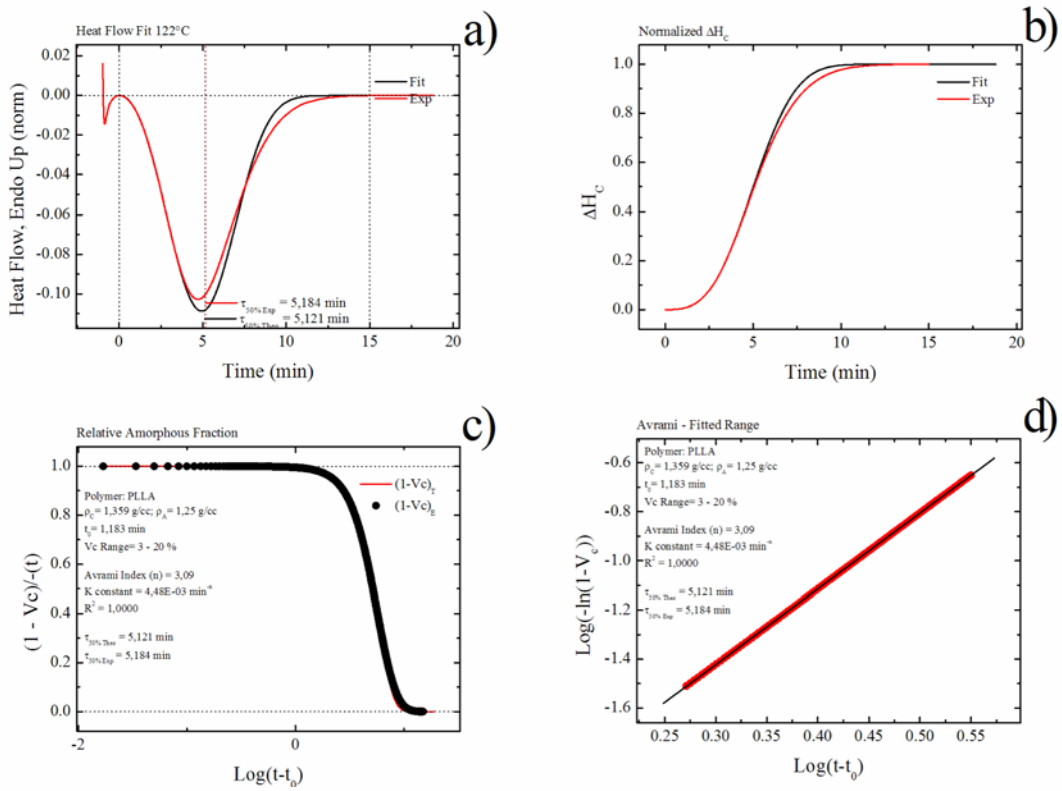

Figure 4.19: Table of Avrami plots obtained by the Origin® plugin developed by Lorenzo *et al* [61]. (a) Experimental DSC crystallization isotherm of PLA/PCL 122°C and its fitting with the Avrami equation. The experimental crystallization half–time is indicated. (b) Relative enthalpy of crystallization as a function of time. (c) Evolution of the normalized volumetric fraction of the amorphous phase as a function of crystallization time. (d) Linear fitting of the Avrami equation in the primary crystallization range, where the slope indicates the Avrami index and the intercept the overall crystallization rate constant

4.11 Effect of PC on the crystallization rate of PLA

Figure 4.18 shows that PLA phase within PLA/PCL/PC reach a crystallization rate fifteen times higher than neat PLA. This effect is not only due to the presence of PCL particles but it derives from a synergistic effect of PC and PCL on PLA, since in PLA/PCL/PC the PLA phase overall crystallization rate is even higher than in PLA/PCL.

Non-isothermal analysis on PLA/PCL/PC indicates that PC does not act as compatibilizers between PLA and PC, since no variation of the Tg of PLA is detected upon the addition of PC in the blend (Fig. 4.13). At the same time, in PLA/PCL/PC the spherulitic growth rate of PLA phase is roughly the same of neat PLA (Figure 4.14). This means that PC does not go to the PLA-PCL interphase, promoting the interpenetration of the chains, but it is dispersed in one or both the phases.

SEM micrographs on PLA/PCL/PC (Figure 4.11e) shows that two kinds of immiscible particles are dispersed in the PLA matrix. One, characterized by larger size, seems to be correspondent to PCL particles and the other one, with lower size, correspondent to PC particles. Therefore, in order to understand the enhancement effect on PLA crystallization rate in the blend upon the addition of PC, we hypothesize that PC, if immiscible with PLA phase could accelerate the PLA crystallization rate by transferring impurities or heterogeneous nuclei.

In order to confirm this hypothesis, a thermal and morphological analysis on binary blends of PLA/PC at weight ratio: 99/1, 98/2, 95/5 was conduced. In this way it is possible to confirm the immiscibility between PLA and PC, and study the effect of PC on the crystallization rate of neat PLA.

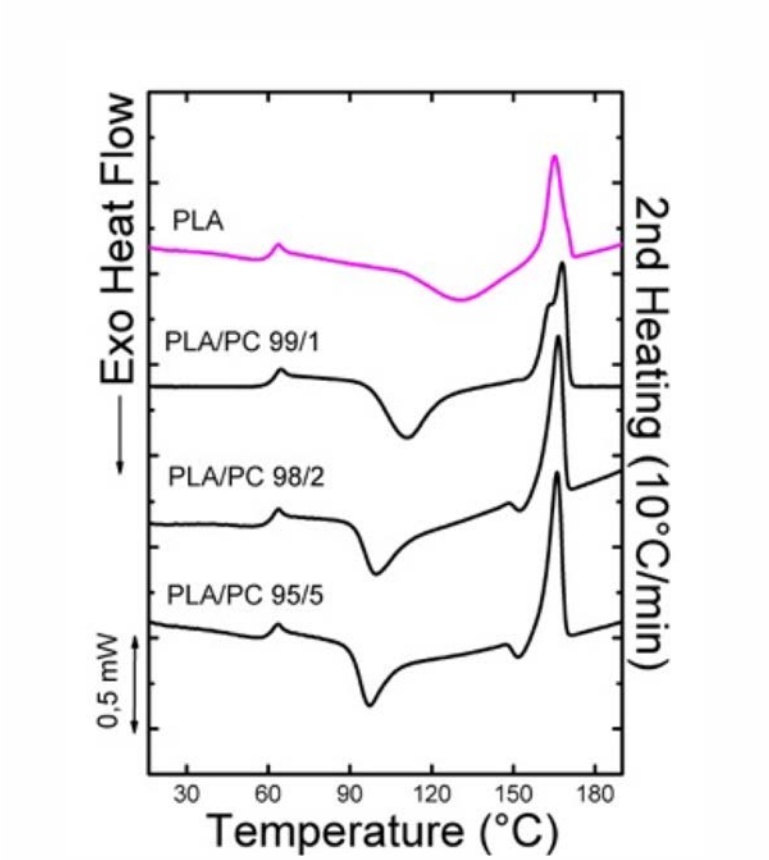

Figure 4.20: Non isothermal DSC experiment on PLA/PC's blend. Second heating curves measured at 10 °C/min.

Non-Isothermal DSC analysis on PLA/PC blends (Figure 4.20) shows that there are no significant variations of Tg of PLA upon blending with PC. At the same time, in SEM micrographs on cryogenically fractured surfaces of PLA/PC blends (Figure 4.12) the typical *sea island morphology* is visible, with PLA conforming the matrix and PC dispersed in droplets.

Isothermal PLOM analysis reveals that PLA spherulitic growth rate is insensible to addiction of PC (Figure 4.21), since PLA and PLA/PC blends are characterized by roughly the same values of G.

This result confirms that, as reported in literature [55] and suggested by previous analysis, PLA and PC are immiscible and PC, not affecting the spherulitic growth rate, could enhance the PLA crystallization rate by only a nucleation effect.

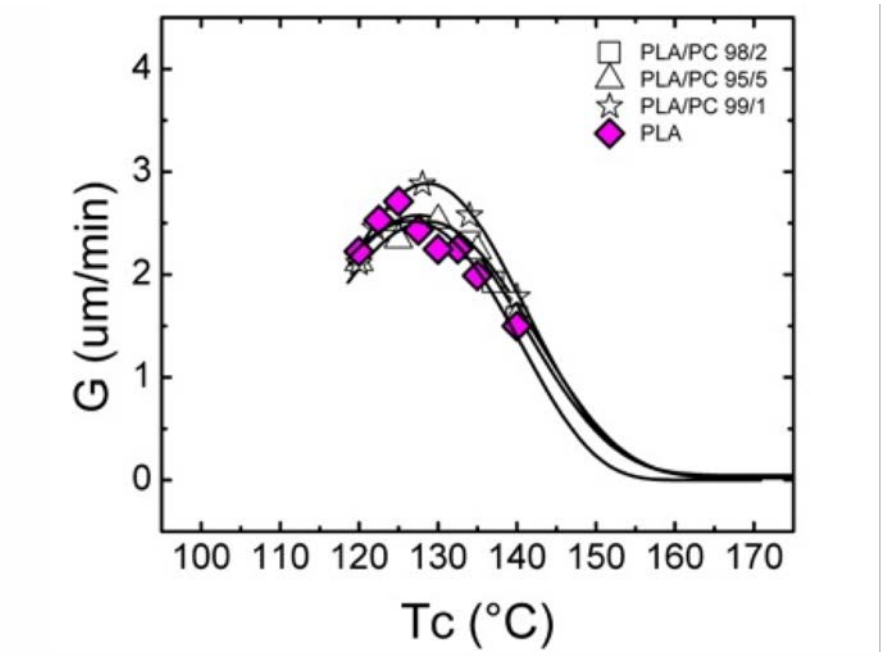

Figure 4.21: Spherulitic growth rate G as a function of isothermal crystallization temperature T_c for neat PLA and PLA phase within PLA/PC's. The solid lines represent arbitrary fits to guide the eye.

Since no significant variation of PLA spherulities growth rate upon blending with PC is detected, it has been decided to investigate the nucleation behaviour of PLA upon blending with PC, after cooling below Tg by an isothermal DSC experiments (Figure 4.22). The analysis was conduced with the same procedure used for PLA/PCL blend.

Fig. 4.22 shows that neat PLA has crystallization rate eight-ten times lower than in PLA/PC blends. Furthermore, the crystallization rate of PLA phase is strictly dependent on the amount of PC in the blend. Increasing the amount of PC from 1 to 5%, crystallization rate is doubled. This result indicates that PC act as nucleating agent for PLA. In PLA/PCL/PC the values of crystallization rate are among the same of PLA/PC blends. This means that in this blend the enhancement effect on crystallization rate of PLA is manly due to the presence of PC.

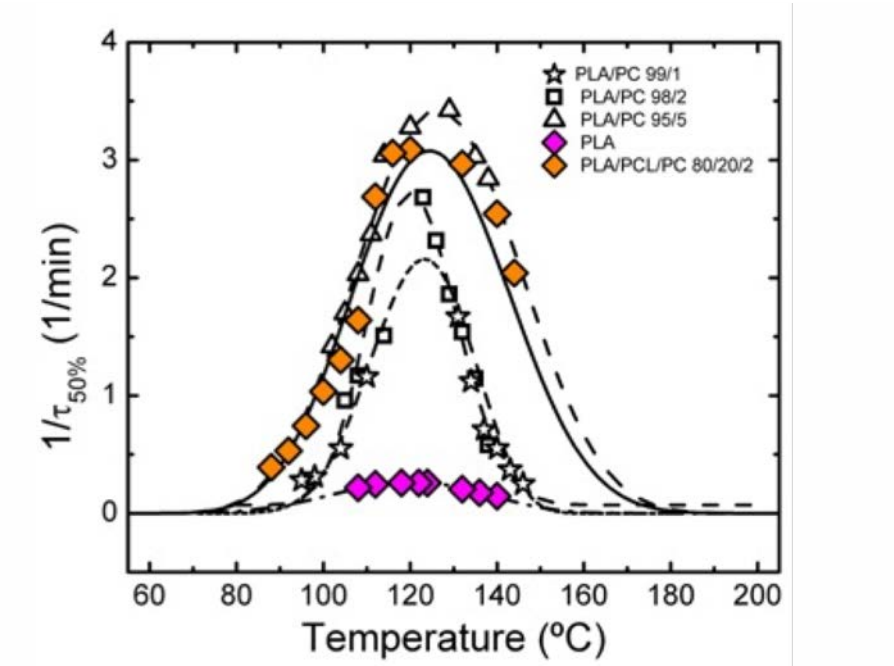

Figure 4.22: Isothermal crystallization experiments conduced from the glassy state. Overall crystallization rate ($1/\tau_{50\%}$) as a function of isothermal crystallization temperature T_c in neat PLA and PLA phase within PLA/PCs blends. The solid lines represent arbitrary fits to guide the eye.

4.12 Annealing DSC experiments

Previous results demonstrated that blending PLA with PCL the isothermal crystallization of PLA is enhanced up to an order of magnitude (see paragraph 4.10). Further addition of P(LA-block-C) copolymers in the blend can tune the crystallization rate of the PLA phase. In PLA/PCL/P(LA-*b*-C)80-20, the PLA phase crystallizes two times faster than PLA/PCL while the addition of P(LA-*b*-C)15-85 gives rise to a sensible reduction of values (Figure 4.18).

The enhancement of PLA isothermal crystallization in PLA/PCL blends is consistent with an acceleration of PLA nucleation, since no significant variation of PLA spherulities growth rate upon blending with PCL is detected (Figure 4.14).

Sakai *et al*. suggest that this nucleation effect derives from an improved miscibility at the PLA-PCL interphase that could induce the formation of active nuclei in PLA phase [42]. However, we disagree with this hypothesis, since to the PLA-PCL blend containing the copolymer with the best compatibilizers action (i.e. P(LA-*b*-C)50-50) does not correspond to the highest crystallization rate.

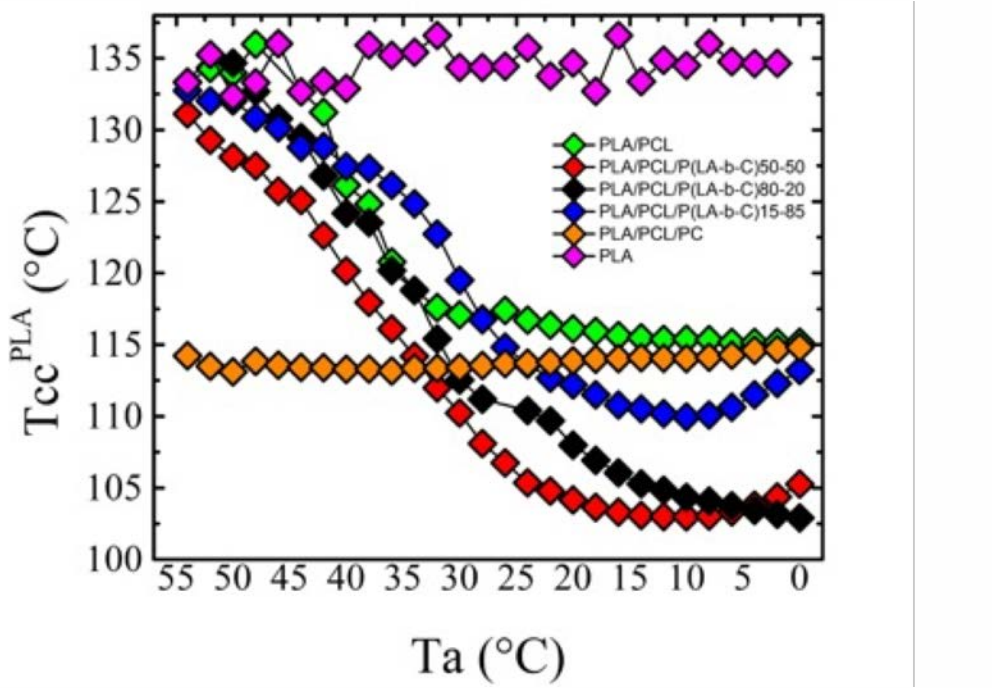

Figure 4.23: Annealing experiment 1. Temperature of cold crystallization (Tcc) of PLA and PLA phase within the blends as a function of the annealing temperature (Ta) employed.

Therefore, in order to elucidate the mechanism that induces the formation of nuclei in the PLA phase of PLA/PCL blends, an annealing test was performed (see paragraph 3.5 - Annealing experiment 1).

Fig. 4.23 shows the PLA temperature of cold crystallization (Tcc) plotted as a function of the annealing temperature (Ta). Tcc of neat PLA does not change reducing Ta, keeping its values always at 135 °C. It means that neat PLA crystallization is insensible to the performed annealing. At the same time in PLA/PCL/PC blend the Tcc of PLA phase does not change reducing the Ta since the nuclei generated by the presence of PC droplets are more effective than PCL in promoting the PLA crystallization, as demonstrated by isothermal analysis on PLA/PCs blends (Figure 4.22).

On the other hand, when PLA is blended with PCL, Tcc of the PLA phase is reduced reducing Ta. It means that PCL could affect the crystallization of the PLA phase. In particular, the Tcc shows a decreasing behaviour by changing the Ta from 54 °C to 30 °C while from 30°C to 0°C the values are almost the same.

This experimental evidence suggests that the crystallization of PCL, that happens in the range from 30 °C to 0 °C, has a pivotal role in the formation of active nuclei that can promote the PLA crystallization. During the rapid cooling

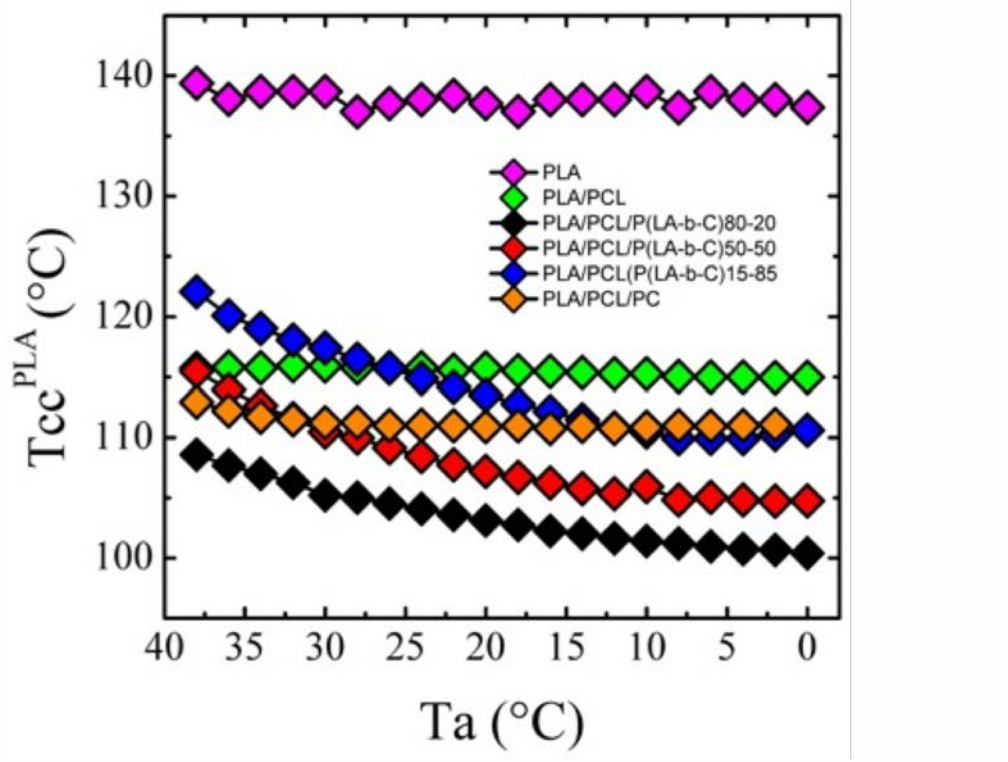

Figure 4.24: Annealing experiment 2. Temperature of cold crystallization (Tcc) of PLA and PLA phase within the blends as a function of the annealing temperature (Ta). Data obtained is referred to the annealing test with PCL phase already crystalline

process of PLA below Tg, the molecular mobility slows down and the material becomes a thermodynamically unstable glass. Meanwhile, during the heating process at an appropriate rate, the unstable and disordered amorphous phase tends to transform into a stable and ordered crystal form. The presence of PCL crystals could induce an orientation of the unstable glass during the cooling below Tg and thus promote the formation of crystals at the PLA-PCL interphase during the subsequent heating scan.

To confirm this hypothesis a second annealing test with PCL phase already crystalline was performed (see paragraph 3.5 – Annealing experiment 2). Figure 4.24 shows data obtained from this second annealing test. For all the blends there is not a significant variation in Tcc upon reducing the annealing temperature, confirming that the PLA nucleation is dependent on the PCL degree of crystallinity. Since PCL is already crystalline, the nucleation effect is almost the same at different annealing temperatures and thus the nucleation enhancement of PLA phase is insensible to the Ta variation.

In order to have a morphological evidence of the described effect a PLOM experiment was conduced. The sample was heated from 25 °C to 200 °C at 20 °C/min and held for 3 minutes to erase the thermal history. Then it was cooled to 20 °C at 60 °C/min and held for another 1 minute. Finally, they were heated at the same speed to the crystallization temperature of 90 °C and held until the crystallization finished (20 min at least). A schematic representation of the thermal steps in function of the time is depicted in Figure 4.25.

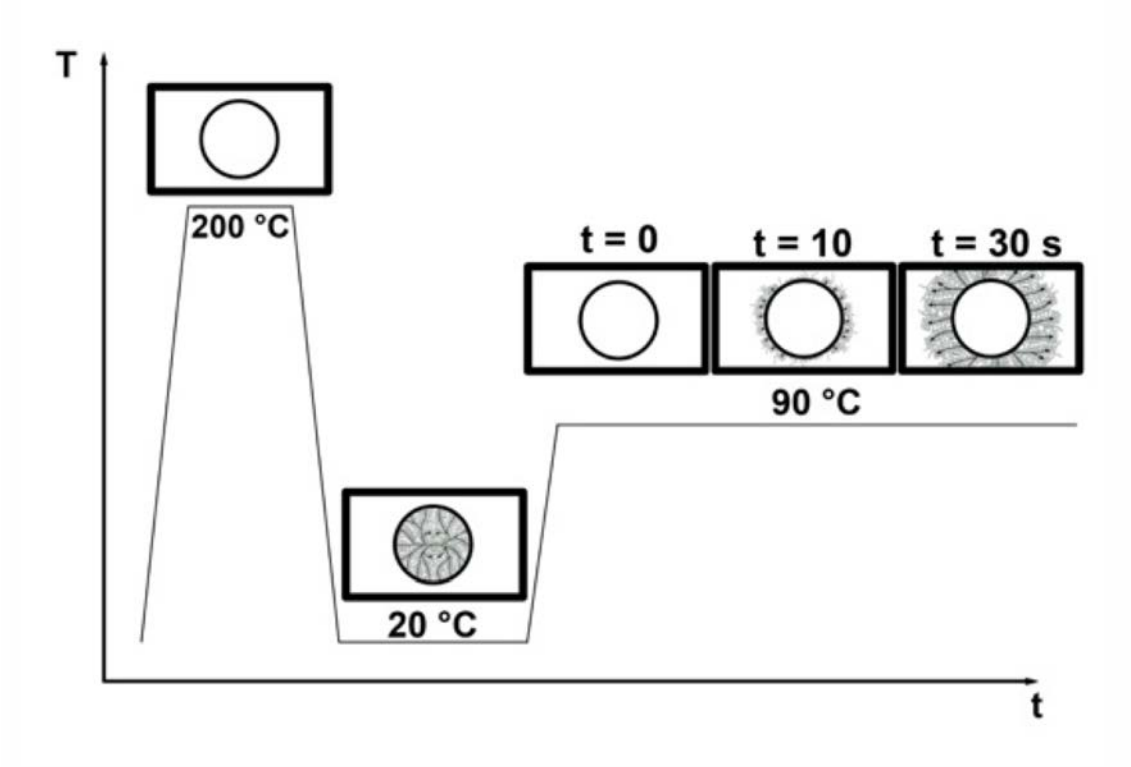

Figure 4.25: Schematic representation of the PLOM experiment performed

Figure 4.26 shows a sequence of images recorded at different times during the isothermal crystallization of PLA phase within PLA/PCL/P(LA-*b*-C)80-20 blend at 90 °C (a schematic draw-representation of the overall process is depicted upward). Images obtained show that the PLA crystals start to growth from the PLA/PCL interphase and proceed trough the entire PLA matrix. When PLA phase completes its crystallization, PLA crystals are mainly distributed at the interphase with PCL droplets and appears as circles, as shown in the micrograph recorded at 30 s. These results clearly shows the PCL droplets induce the formation of PLA crystals

The experimental evidences obtained here suggest that the differences among the crystallization rates of PLA phases within the PLA/PCL blends are correlated

to the different degree of crystallinity of the PCL phases. The presence of PCL crystals could induce an orientation of the unstable glass PLA chains during the cooling below Tg and thus promote the formation of crystals at the PLA-PCL interphase during the subsequent heating scan.

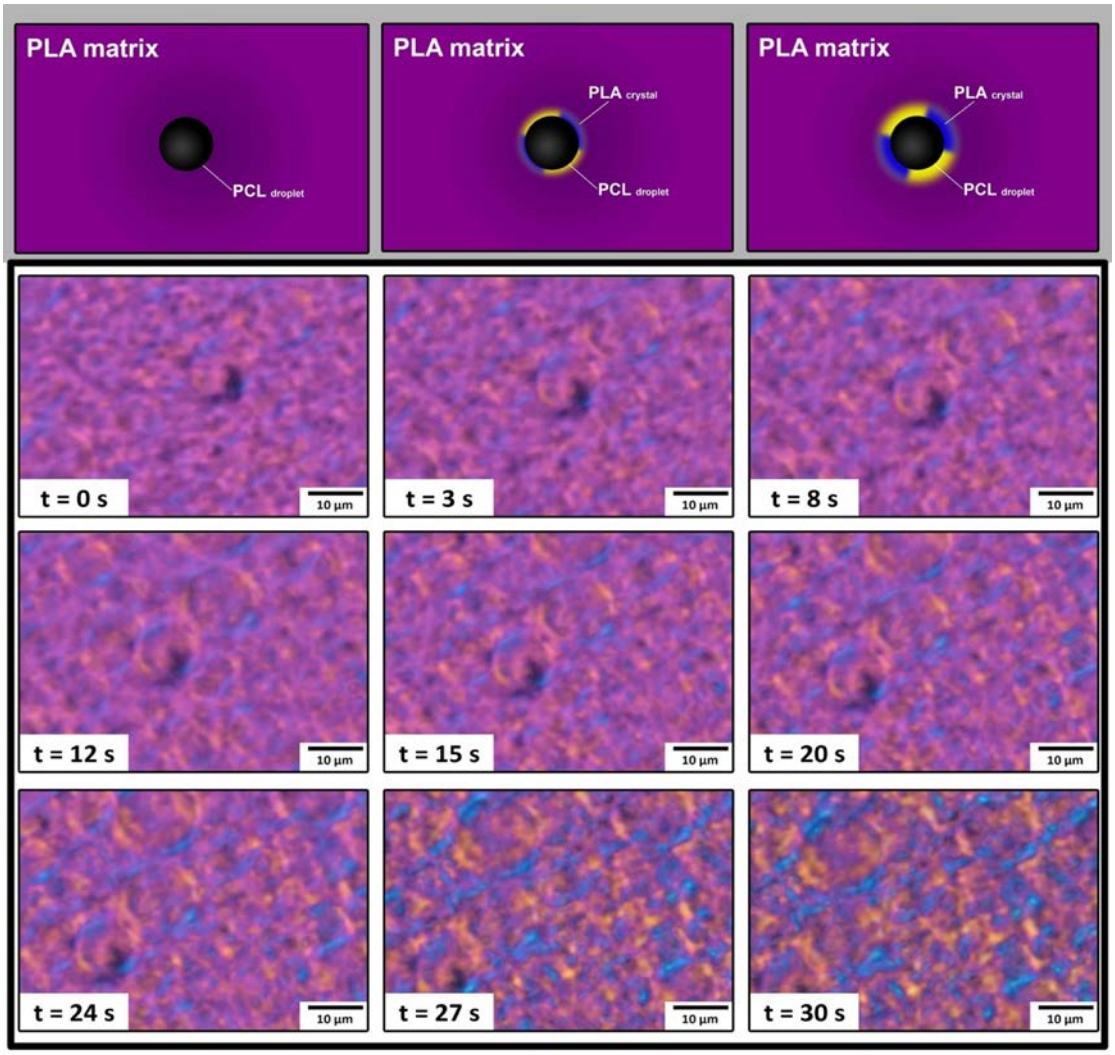

Figure 4.26: PLOM micrographs recorded at different times during the crystallization of PLA phase with PLA/PCL/P(LA-*b*-C)80-20 blend at 90 °C.

If this hypothesis is true, the crystallization rate of PLA must be correlated with the PCL enthalpy of melting within the blends, as it reflects the amount of PCL crystals that could induce the formation of active nuclei.

Figure 4.27 shows the heating scan after the cooling at 60°C/min to 20°C of previous isothermal DSC experiments on PLA/PCL blends while in Table 4.8 are reported the melting area of PCL phase.

The blend with the highest crystallization rate (i.e: PLA/PCL/P(LA-*b*-C)80-20) of the PLA phase is the one that, according to the Table 4.8, has the highest enthalpy of melting for the PCL phase.

While the blend with lowest crystallization rate (i.e: PLA/PCL/P(LA-*b*-C)15-85) of the PLA phase has the lowest enthalpy of melting for the PCL phase.

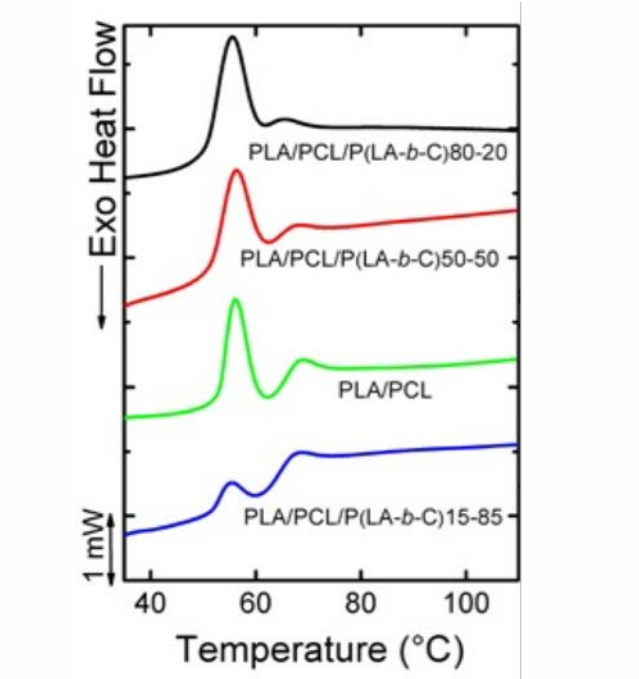

Figure 4.27: Isothermal DSC experiment from the glassy state. Second heating curves at 20 °C/min. The curves have been normalized by the weight of the samples

Table 4.8: PCL enthalpy of melting recorded during second heating at 20 °C/min. The enthalpies of melting have been normalized by the weight fraction of the sample

	Comp. (w/w)	PCL ΔHm (J/g)
PLA/PCL	80/20	3.26
PLA/PCL/P(LA-*b*-C)80-20	80/20/2	5.18
PLA/PCL/P(LA-*b*-C)50-50	80/20/2	3.89
PLA/PCL/P(LA-*b*-C)15-85	80/20/2	0.89

The different degree of crystallinity of PCL within the blends is related to the amount of PC block in the copolymers due to a reported miscibility between PCL and PC (Flory-Huggins interaction parameter between -1 and -2 [71][72]). As reported in literature [68], PC can interact with PCL droplets when it is present as blocky units into P(LA-*b*-C) copolymers reducing the chains mobility and shifting the crystallization of PCL at lower temperatures.

5 CONCLUSIONS

In this work poly(L-lactide)-poly(carbonate) block copolymers were synthetized by ring opening polymerization (ROP) in three different compositions using purified commercial L-lactide and PC oligomers previously synthetized. The block copolymers were characterized by spectroscopic and thermal analyses. DSC and TGA experiments confirm that PLA and PC blocks within the copolymers are immiscible after the precipitation in methanol but became miscible if heated at the melt state. ^{1}H-NMR and ATR analyses suggest the presence of copolymers with blocky structure composed by poly(lactide) and poly(carbonate) as repeating units.

The compatibilization effect of poly(lactide-*block*-carbonate) was evaluated upon blending with poly(lactide)/poly(ε-caprolactone) (PLA/PCL) 80/20 blend by morphological and thermal analyses and the results were compared with neat PLA, PCL and a blend containing PC as compatibilizer.

The P(LA-*b*-C) block copolymer characterized by the same amount of PLA and PC (indicated as P(LA-*b*-C)50-50) is the best one for compatibilizing the PLA/PCL blend. In fact, upon its addition the highest reduction of PCL particles diameter and of PLA Tg depression was obtained. These results were correlated with the spherulitic growth rate of PLA phase within the blends evaluated by PLOM experiments.

Isothermal DSC experiments shows that the isothermal cold crystallization of the PLA phase is enhanced upon blending with PCL and a further crystallization enhancement is observed when both P(LA-*b*-C) copolymers and PC are added. In particular the presence of PC could be effective as a nucleation agent for the PLA phase, increasing the PLA crystallization rate more that one order of magnitude.

Annealing experiments demonstrated that the crystallization of the PCL phase induces the formation of active nuclei in PLA when cooled below Tg. In fact, as a result, the crystallization rate of PLA depends on the capacity of PCL to crystallize within the blend. The copolymers with the higher amount of PC, inhibit the crystallization of PCL and, thus, reduce the crystallization rate of PLA.

6 REFERENCES

[1] Rosen, S. L. (1982). *Fundamental principles of polymeric materials*. Wiley.

[2] Tokiwa, Y., Calabia, B. P., Ugwu, C. U., & Aiba, S. (2009). Biodegradability of plastics. *International journal of molecular sciences*, *10*(9), 3722-3742.

[3] Mark, H. F. (2013). *Encyclopedia of polymer science and technology, concise*. John Wiley & Sons.

[4] Olabis, O. (2012). *Polymer-polymer miscibility*. Elsevier.

[5] Lorenzo, A. T., & Müller, A. J. (2008). Estimation of the nucleation and crystal growth contributions to the overall crystallization energy barrier. *Journal of Polymer Science Part B: Polymer Physics*, *46*(14), 1478-1487.

[6] Mandelkern, L. (1964). *Crystallization of polymers* (Vol. 38). New York: McGraw-Hill.

[7] Avrami, M. (1941). Kinetics of phase change. III. Granulation, phase change, and microstructure. *J. Chem. Phys*, *9*(2), 177-184.

[8] Piemonte, V., Sabatini, S., & Gironi, F. (2013). Chemical recycling of PLA: a great opportunity towards the sustainable development?. *Journal of Polymers and the Environment*, *21*(3), 640-647.

[9] Auras, R., Harte, B., & Selke, S. (2004). An overview of polylactides as packaging materials. *Macromolecular bioscience*, *4*(9), 835-864.

[10] Auras, R., Lim, L. T., Selke, S. E., & Tsuji, H. (Eds.). (2011). *Poly (lactic acid): synthesis, structures, properties, processing, and applications* (Vol. 10). John Wiley & Sons.

[11] Hamad, K., Kaseem, M., Yang, H. W., Deri, F., & Ko, Y. G. (2015). Properties and medical applications of polylactic acid: A review. *Express Polymer Letters*, *9*(5), 435-455.

[12] Hartmann, M. H. (1998). High molecular weight polylactic acid polymers. In *Biopolymers from renewable resources* (pp. 367-411). Springer Berlin Heidelberg.

[13] Lunt, J. (1998). Large-scale production, properties and commercial applications of polylactic acid polymers. *Polymer degradation and stability*, *59*(1), 145-152.

[14] Garlotta, D. (2001). A literature review of poly (lactic acid). *Journal of Polymers and the Environment*, *9*(2), 63-84.

[15] Nijenhuis, A. J., Grijpma, D. W., & Pennings, A. J. (1991). Highly crystalline as-polymerized poly (L-lactide). *Polymer Bulletin*, *26*(1), 71-77.Polymer 1980, 21,

607.

[16] Huang, J., Lisowski, M. S., Runt, J., Hall, E. S., Kean, R. T., Buehler, N., & Lin, J. S. (1998). Crystallization and microstructure of poly (l-lactide-co-meso-lactide) copolymers. *Macromolecules*, *31*(8), 2593-2599.

[17]Fischer, E. W., Sterzel, H. J., & Wegner, G. K. Z. Z. (1973). Investigation of the structure of solution grown crystals of lactide copolymers by means of chemical reactions. *Kolloid-Zeitschrift und Zeitschrift für Polymere*, *251*(11), 980-990.

[18] Saeidlou, S., Huneault, M. A., Li, H., & Park, C. B. (2012). Poly (lactic acid) crystallization. *Progress in Polymer Science*, *37*(12), 1657-1677.

[19] Na, B., Zou, S., Lv, R., Luo, M., Pan, H., & Yin, Q. (2011). Unusual cold crystallization behavior in physically aged poly (L-lactide). *The Journal of Physical Chemistry B*, *115*(37), 10844-10848.

[20] Lv, S., Gu, J., Cao, J., Tan, H., & Zhang, Y. (2015). Effect of annealing on the thermal properties of poly (lactic acid)/starch blends. *International journal of biological macromolecules*, *74*, 297-303.

[21] Porter, K. A. (2006). Ring Opening Polymerization of Lactide for The synthesis of Poly (Lactic Acid). *State of Illinois*.

[22] Stevens, M. P. (1990). *Polymer chemistry* (Vol. 2). New York: oxford university press.

[23] Brunelle, D. J., & Korn, M. R. (2005). *Advances in polycarbonates*. American Chemical Society; Distributed by Oxford University Press.

[24] Christopher, W. F., & Fox, D. W. (1962). *Polycarbonates* (Vol. 24). Reinhold Publishing Corporation.

[25] Delimoy, D., Goffaux, B., Devaux, J., & Legras, R. (1995). Thermal and morphological behaviours of bisphenol A polycarbonate/poly (butylene terephthalate) blends. *Polymer*, *36*(17), 3255-3266.

[26] Zhang, X., Xie, F., Pen, Z., Zhang, Y., Zhang, Y., & Zhou, W. (2002). Effect of nucleating agent on the structure and properties of polypropylene/poly (ethylene–octene) blends. *European Polymer Journal*, *38*(1), 1-6.

[27] Liu, C., Lin, S., Zhou, C., & Yu, W. (2013). Influence of catalyst on transesterification between poly (lactic acid) and polycarbonate under flow field. *Polymer*, *54*(1), 310-319.

[28] Paul, D. R., & Barlow, J. W. (1980). Polymer blends. *Journal of Macromolecular Science—Reviews in Macromolecular Chemistry*, *18*(1), 109-168.

[29] Nijenhuis, A. J., Colstee, E., Grijpma, D. W., & Pennings, A. J. (1996). High molecular weight poly (L-lactide) and poly (ethylene oxide) blends: Thermal characterization and physical properties. *Polymer*, *37*(26), 5849-5857.

[30] Li, F. J., Zhang, S. D., Liang, J. Z., & Wang, J. Z. (2015). Effect of polyethylene glycol on the crystallization and impact properties of polylactide-based blends. *Polymers for Advanced Technologies*, *26*(5), 465-475.

[31] Puppi, D., Chiellini, F., Piras, A. M., & Chiellini, E. (2010). Polymeric materials for bone and cartilage repair. *Progress in Polymer Science*, *35*(4), 403-440.

[32] López-Rodríguez, N., López-Arraiza, A., Meaurio, E., & Sarasua, J. R. (2006). Crystallization, morphology, and mechanical behavior of polylactide/poly (ε-caprolactone) blends. *Polymer Engineering & Science*, *46*(9), 1299-1308.

[33] Wu, D., Zhang, Y., Zhang, M., & Zhou, W. (2008). Phase behavior and its viscoelastic response of polylactide/poly (ε-caprolactone) blend. *European Polymer Journal*, *44*(7), 2171-2183.

[34] David, D. J., & Sincock, T. F. (1992). Estimation of miscibility of polymer blends using the solubility parameter concept. *Polymer*, *33*(21), 4505-4514.

[35] Zeng, J. B., Li, K. A., & Du, A. K. (2015). Compatibilization strategies in poly (lactic acid)-based blends. *Rsc Advances*, *5*(41), 32546-32565.

[36] Koning, C., Van Duin, M., Pagnoulle, C., & Jerome, R. (1998). Strategies for compatibilization of polymer blends. *Progress in Polymer Science*, *23*(4), 707-757.

[37] Choi, N. S., Kim, C. H., Cho, K. Y., & Park, J. K. (2002). Morphology and hydrolysis of PCL/PLLA blends compatibilized with P (LLA-co-єCL) or P (LLA-b-єCL). *Journal of applied polymer science*, *86*(8), 1892-1898.

[38] Utracki, L. A., & Wilkie, C. A. (Eds.). (2002). *Polymer blends handbook* (Vol. 1, p. 2). Dordrecht, The Netherlands: Kluwer Academic Publishers.

[39] Sheth, M., Kumar, R. A., Davé, V., Gross, R. A., & McCarthy, S. P. (1997). Biodegradable polymer blends of poly (lactic acid) and poly (ethylene glycol). *Journal of Applied Polymer Science*, *66*(8), 1495-1505.

[40] Pillin, I., Montrelay, N., & Grohens, Y. (2006). Thermo-mechanical characterization of plasticized PLA: Is the miscibility the only significant factor?. *Polymer*, *47*(13), 4676-4682.

[41] Rizzuto, M., Mugica, A., Zubitur, M., Caretti, D., & Müller, A. J. (2016). Plasticization and anti-plasticization effects caused by poly (lactide-ran-caprolactone) addition to double crystalline poly (l-lactide)/poly (ε-caprolactone) blends. *CrystEngComm*, *18*(11), 2014-2023.

[42] Sakai, F., Nishikawa, K., Inoue, Y., & Yazawa, K. (2009). Nucleation enhancement effect in poly (l-lactide)(PLLA)/poly (ε-caprolactone)(PCL) blend

induced by locally activated chain mobility resulting from limited miscibility. *Macromolecules*, *42*(21), 8335-8342.

[43] Dell'Erba, R., Groeninckx, G., Maglio, G., Malinconico, M., & Migliozzi, A. (2001). Immiscible polymer blends of semicrystalline biocompatible components: thermal properties and phase morphology analysis of PLLA/PCL blends. *Polymer*, *42*(18), 7831-7840.

[44] Brunelle, D. J. (2005). Advances in polycarbonates: An overview. In *ACS symposium series* (Vol. 898, pp. 1-5). Oxford University Press.

[45] Ostafinska, A., Fortelny, I., Nevoralova, M., Hodan, J., Kredatusova, J., & Slouf, M. (2015). Synergistic effects in mechanical properties of PLA/PCL blends with optimized composition, processing, and morphology. *RSC Advances*, *5*(120), 98971-98982.

[46] Luyt, A. S., & Gasmi, S. (2016). Influence of blending and blend morphology on the thermal properties and crystallization behaviour of PLA and PCL in PLA/PCL blends. *Journal of Materials Science*, *51*(9), 4670-4681.

[47] Fortelný, I., Ostafińska, A., Michálková, D., Jůza, J., Mikešová, J., & Šlouf, M. (2015). Phase structure evolution during mixing and processing of poly (lactic acid)/polycaprolactone (PLA/PCL) blends. *Polymer Bulletin*, *72*(11), 2931-2947.

[48] Urquijo, J., Guerrica-Echevarría, G., & Eguiazábal, J. I. (2015). Melt processed PLA/PCL blends: Effect of processing method on phase structure, morphology, and mechanical properties. *Journal of Applied Polymer Science*, *132*(41).

[49] Ostafinska, A., Fortelny, I., Nevoralova, M., Hodan, J., Kredatusova, J., & Slouf, M. (2015). Synergistic effects in mechanical properties of PLA/PCL blends with optimized composition, processing, and morphology. *RSC Advances*, *5*(120), 98971-98982.

[50] Arnal, M. L., Matos, M. E., Morales, R. A., Santana, O. O., & Müller, A. J. (1998). Evaluation of the fractionated crystallization of dispersed polyolefins in a polystyrene matrix. *Macromolecular Chemistry and Physics*, *199*(10), 2275-2288.

[51] Kim, J., Gracz, H. S., Roberts, G. W., & Kiserow, D. J. (2008). Spectroscopic analysis of poly (bisphenol A carbonate) using high resolution 13 C and 1 H NMR. *Polymer*, *49*(2), 394-404.

[52] Parshin, A. M., Gunyakov, V. A., Zyryanov, V. Y., & Shabanov, V. F. (2013). Domain structures in nematic liquid crystals on a polycarbonate surface.*International journal of molecular sciences*, *14*(8), 16303-16320.

[53] Bendler, J. T. (Ed.). (1999). *Handbook of polycarbonate science and technology*. CRC Press.

[54] Williams, M. L., Landel, R. F., & Ferry, J. D. (1955). The temperature dependence of relaxation mechanisms in amorphous polymers and other glass-forming liquids. *Journal of the American Chemical society*, *77*(14), 3701-3707.

[55] Liu, C., Lin, S., Zhou, C., & Yu, W. (2013). Influence of catalyst on transesterification between poly (lactic acid) and polycarbonate under flow field. *Polymer*, *54*(1), 310-319.

[56] Chen, C. C., Chueh, J. Y., Huang, H. M., & Lee, S. Y. (2003). Preparation and characterization of biodegradable PLA polymeric blends. *Biomaterials*, *24*(7), 1167-1173.

[57] Jang, B. N., & Wilkie, C. A. (2004). A TGA/FTIR and mass spectral study on the thermal degradation of bisphenol A polycarbonate. *Polymer Degradation and Stability*, *86*(3), 419-430.

[58] Matta, A. K., Rao, R. U., Suman, K. N. S., & Rambabu, V. (2014). Preparation and characterization of biodegradable PLA/PCL polymeric blends. *Procedia Materials Science*, *6*, 1266-1270.

[59] Chavalitpanya, K., & Phattanarudee, S. (2013). Poly (lactic acid)/polycaprolactone blends compatibilized with block copolymer. *Energy Procedia*, *34*, 542-548.

[60] Favis, B. D., & Willis, J. M. (1990). Phase size/composition dependence in immiscible blends: experimental and theoretical considerations. *Journal of Polymer Science Part B: Polymer Physics*, *28*(12), 2259-2269.

[61] Lorenzo, A. T., Arnal, M. L., Albuerne, J., & Müller, A. J. (2007). DSC isothermal polymer crystallization kinetics measurements and the use of the Avrami equation to fit the data: guidelines to avoid common problems. *Polymer testing*, *26*(2), 222-231.

[62] Inoue, T. (2003). Morphology of polymer blends. In *Polymer Blends Handbook* (pp. 547-576). Springer Netherlands.

[63] Michell, R. M., Blaszczyk-Lezak, I., Mijangos, C., & Müller, A. J. (2013). Confinement effects on polymer crystallization: from droplets to alumina nanopores. *Polymer*, *54*(16), 4059-4077.

[64] Jiménez, A., Peltzer, M., & Ruseckaite, R. (Eds.). (2014). *Poly (lactic acid) Science and Technology: Processing, Properties, Additives and Applications* (No. 12). Royal Society of Chemistry.

[65] McCrum, N. G., Buckley, C. P., & Bucknall, C. B. (1997). *Principles of polymer engineering*. Oxford University Press, USA.

[66] Guo, Q. (2016). *Polymer Morphology: Principles, Characterization, and Processing*. John Wiley & Sons.

[67] Michell, R. M., & Müller, A. J. (2016). Confined crystallization of polymeric materials. *Progress in Polymer Science*, *54*, 183-213.

[68] Balsamo, V., Calzadilla, N., Mora, G., & Müller, A. J. (2001). Thermal characterization of polycarbonate/polycaprolactone blends. *Journal of Polymer Science Part B: Polymer Physics*, *39*(7), 771-785.

[69] López-Rodríguez, N., López-Arraiza, A., Meaurio, E., & Sarasua, J. R. (2006). Crystallization, morphology, and mechanical behavior of polylactide/poly (ε-caprolactone) blends. *Polymer Engineering & Science*, *46*(9), 1299-1308.

[70] A. T. Lorenzo, "Avrami and LH Plugin for Origin" (2013). Available at: https://sites.google.com/a/usb.ve/ajmuller/downloads/plugins

[71] Chun, Y. S., Park, J., Sun, J. B., & Kim, W. N. (2000). Blends of polycarbonate and poly (ϵ-caprolactone) and the determination of the polymer–polymer interaction parameter of the two polymers. *Journal of Polymer Science Part B: Polymer Physics*, *38*(15), 2072-2076.

[72] Varnell, D. F., Runt, J. P., & Coleman, M. M. (1981). Fourier transform infrared studies of polymer blends. 4. Further observations on the poly (bisphenol A carbonate)-poly (iε-caprolactone) system. *Macromolecules*, *14*(5), 1350-1356.